

Impact of Varying Collision Avoidance Strategies on Human Stress Level in Human-Robot Interaction

Master Thesis

submitted to

Institute of Control Theory and Systems Engineering

Faculty of Electrical Engineering and Information Technology

Technische Universität Dortmund

by

Mohammed Faizan

Chennai, India

Date of Submission: February 11, 2024

Responsible Professor:

Univ.-Prof. Dr.-Ing. Prof. h.c. Dr. h.c. Torsten Bertram

Academic Supervisors:

M.Sc. Heiko Renz

M.Sc. Khazar Dargahi Nobari

“Das ist die Widmung / This is the dedication (optional)”

Acknowledgement

Das ist die Danksagung / This is the acknowledgement (optional)

Abstract

Das ist die Kurzfassung (siehe Abschnitt ??) / This is the abstact (see section ??).

Contents

Nomenclature	ii
1 Introduction	1
1.1 Motivation ^{†_{MO}}	1
1.2 Aim of the Thesis ^{†_{MO}}	2
1.3 Related Work	3
1.4 Structure of the Thesis	3
2 Theoretical foundation	4
2.1 Stress Definition and Measurement	4
2.2 Subjective Measures ^{†_{MO}}	5
2.3 Objective Measures ^{†_{MO}}	6
2.3.1 Empatica E4	6
2.3.2 Motion Capture	10
2.4 UR10 robot and Collision Avoidance ^{†_{MO}}	10
2.5 Stress Classification ^{†_{MG}}	13
3 Data Collection-Subject Study	18
3.1 Design of Tasks	18
3.2 Apparatus and Experimental Setup	20
3.3 Experimental Procedure	22
4 Stress Detection Methodology	25
4.1 Data Synchronization ^{†_{MO}}	25
4.2 Pre-Processing ^{†_{MO}}	26
4.3 Feature Extraction ^{†_{MO}}	28
4.3.1 BVP-Blood Volume Pressure	29
4.3.2 EDA-Electrodermal Activity	31
4.3.3 Body Features	33
4.4 Ground Truth	36
4.5 Classification /Stress Detection/	36
5 Result	38
6 Discussion and Conclusion	39
Bibliography	40
7 Appendix	44
7.1 Usage of generative AI - Affidavit	45

Nomenclature

Greek symbols

Abbreviations and Acronyms

BVP	Blood Volume Pressure
Cobots	Collaborative Robots
EDA	Electrodermal Activity
GMM	Gaussian Mixture Model
GSR	Galvanic Skin Response
HR	Heart Rate
HRV	Heart Rate Variability
KNN	K-Nearest Neighbors
MPC	Model Predictive Control
NASA-TLX	National Aeronautics Space Administration–Task Load Index
PPG	Photoplethysmography
PSS	Perceived Stress Scale
SAM	Self-Assessment Manikin
SVM	Support Vector Machines

Usage of generative AI models

- \ddagger_{MO} Media optimization: Correction, optimization, or restructuring of entire passages
 \ddagger_{MG} Media generation: Creating entire passages from given content.

Explanations for the usage of generative AI models and its notation:

The bottommost level at which the identification is presented regarding the possible uses of generative AI models are subchapters of the 2nd order (e.g., 1.1.1, which may also appear without numbering), as otherwise, the identification would disrupt the reading flow due to frequent occurrences. Algorithms used for implementing generative AI models are mentioned at least in the text or provided as pseudo-code to facilitate appropriate identification.

1

Introduction

1.1 Motivation †MO

Industry 4.0, also known as the Fourth Industrial Revolution, has brought about significant transformations, particularly in the manufacturing sector. This revolution has been characterized by the introduction of intelligent technologies such as the Internet of Things (IoT), cloud connectivity, big data, and human-robot collaboration. These advancements have led to notable improvements and innovations, with the core principle and driving force of innovation in Industry 4.0 being the enhancement of efficiency and productivity. Human-robot collaboration, a key component of Industry 4.0, has played a massive role in this advancement by bringing humans closer together and facilitating more efficient and cooperative workflows.

Traditionally, industrial robots like robot manipulators, autonomous mobile robots, and gantry models have been kept separate from human workers primarily due to safety concerns. These robots, with their large size, substantial weight, and high speed, pose potential hazards when in close proximity to humans. This traditional approach prioritized the physical separation of robots and humans in industrial settings. However, advancements in Industry 4.0 have significantly increased the use of collaborative robots (cobots), bringing them closer together to accomplish tasks jointly. This evolutionary progression has witnessed the transformation of robots from being secluded behind safety barriers to now operating side-by-side with their human counterparts, effectively capitalizing on their unique capabilities which combine human adaptability and decision-making skills with the precision and consistency offered by robots.

Looking towards the future of the emerging Industry 5.0, the focus shifts towards a more human-centric approach (Pereira and Santos 2023). Industry 5.0 aims to strike a balance between technological advancements and human needs and interests. The goal is to merge the technological efficiency of Industry 4.0 with a greater emphasis on enhancing human operator's well-being and satisfaction. Industry 5.0 aims to address the human challenges of Industry 4.0 as a human-centric solution, placing the worker's well-being at the centre of the production process (Nahavandi 2019). This shows a significant shift from purely efficiency-driven operations to those that also prioritize human factors and environmental sustainability.

With a focus on the human centrism aspect of Industry 5.0, this thesis aims to delve into

the human aspect of human-robot interaction, considering how proximity to robots might affect the operator's physiological state. It aims to investigate how continuous interaction with robots impacts the stress levels experienced by humans and emphasizes the importance of monitoring and accurately assessing stress levels in human-robot collaborative environments. Sauppé and Mutlu (2015) have previously indicated that cobots have the ability to influence the mental states of human workers, as they are often perceived as social entities. The close proximity of humans to robots in the workplace can lead to heightened stress levels, mainly if the robot's movements appear to be potentially harmful (Lasota and Shah 2015). For instance, if a co-robot swiftly moves towards a worker or follows an unpredictable path, it may induce feelings of anxiety or fear due to the perceived risk of sustaining an injury. This, in turn, can negatively impact both productivity and the efficacy of human-robot collaboration. Furthermore, it can impede the complete utilization of the advanced capabilities offered by collaborative robots. As robots become more autonomous and capable, identifying and addressing these stress factors is critical to optimizing human-robot collaboration for enhanced productivity and making the working environment effective, efficient and safe.

1.2 Aim of the Thesis^{†MO}

The primary objective of this thesis is to evaluate the impact of varying collision avoidance strategies on human stress levels within the context of human-robot interaction. This involves conducting a study to collect and analyze data, aiming to understand the varying stress levels concerning different robot collision avoidance strategies while considering various collaboration levels and robot control strategies. Subsequently, the data obtained is utilized to develop a predictive model capable of identifying and addressing sources of stress during human-robot collaboration.

Specifically, the primary objectives of the thesis are:

- **Assessment of Human Stress Levels :** Develop a holistic approach for evaluating stress levels in human-robot interactions during different collaboration levels and robot control strategies, combining both objective physiological measures and subjective experiences. Objectively, the study will employ various physiological indicators such as Galvanic Skin Response (GSR), Electrodermal Activity (EDA), Heart Rate (HR), and body posture analysis. These indicators will provide quantifiable data on the body's physiological response to robot interactions. Subjectively, the study aims to incorporate personal feedback from participants gathered through questionnaires. This will offer insights into their personal feelings and perceptions regarding their interactions with robots. By blending these objective and subjective methods, the study aims to understand stress in human-robot interactions comprehensively. This entails designing an acquisition system that successfully takes data from several sensors at different frequencies and synchronizes it. Devices such as the Empatica E4 wristband are used for gathering data on GSR, EDA, and other parameters, as well as a motion capture system to record human posture and movement. A vital aspect would be to synchronize these many data streams, ensuring accurate and consistent assessment of human physiological states across different robot interaction

scenarios. An important aspect was designing and conducting a subject study to collect data on participants' physiological responses while doing different assembly tasks under different human-robot interaction scenarios. These scenarios included three distinct levels of robot collision avoidance strategies: No collision avoidance, dynamic collision avoidance, and predictive collision avoidance, as well as three different collaboration levels: separated workspace with the cobot, shared workspace, and shared workspace with direct collaboration. The aim is to gather comprehensive data to analyze the impact of these varying robot control strategies on human stress levels.

- **Stress Prediction Model:** Developing a model for predicting and classifying stress levels during human-robot collaboration. This model trained on the dataset of human physiological responses collected from the subject study. Various preprocessing and feature engineering techniques are used to prepare the data for the model. Various machine learning models, such as K-Nearest Neighbors (KNN), Support Vector Machines (SVM), and others, are evaluated to determine the best model for predicting stress levels. The ultimate goal of this model is to provide a reliable tool for real-time monitoring and assessment of stress levels during human-robot collaboration. Accurately identifying stress-inducing factors and patterns can contribute to the development of proactive interventions and collision avoidance strategies that can enhance the overall well-being and performance of individuals engaged in human-robot interaction scenarios.

1.3 Related Work

1.4 Structure of the Thesis

In Chapter 2, we delve into the fundamental concepts of stress and examine the relationship between stress and key physiological signals such as EDA, HR and GSR. Chapter 3 describes the data collection process of the subject study that was conducted to collect data on participants' physiological responses. Chapter 4 describes the data analysis process of the subject study to analyze the collected data and the different pre-processing techniques and feature selection used to build the model. Chapter 5 describes the results of the subject study and the different machine learning models that were evaluated to determine the best model for predicting stress levels. Chapter 6 concludes the thesis and outlines the future work and research directions.

2

Theoretical foundation

2.1 Stress Definition and Measurement

Stress, a term frequently used in everyday language as well as in scientific domain, is an individual's response to situations perceived as challenging, threatening, or overwhelming. Stress is an unpleasant emotional state that individuals experience when confronted with demands that they perceive as taxing or exceeding their coping capabilities (Lee et al. 2004).

Stress, also called the "fight-or-flight" response, is an evolutionary adaptation that equips someone to respond to demanding situations rapidly. When faced with a potential threat or challenge, the human body instinctively readies itself for self-defence or swift evasion. The body's sympathetic nervous system is responsible for this response, which rapidly increases the production of stress hormones like cortisol, adrenaline, and noradrenaline (Gedam and Paul 2021).

The hormonal changes cause a range of bodily reactions, including acceleration of the heartbeat, muscle tension, changes in posture, increased blood pressure, rapid breathing, and heightened sensory alertness etc. One can objectively measure these bodily changes, which generally fall into two categories: physical and physiological changes.

Physical measures focus on observable bodily changes that occur under stress. These include alterations in facial expressions, variations in the rate of eye blinking and pupil dilation, changes in body posture and movement patterns. These visible markers offer insights into an individual's stress levels.

Physiological measures, in contrast, involve using sensors to detect internal bodily changes indicative of stress. A range of biomarkers is employed for this purpose, including Heart Rate Variability (HRV) and HR, GSR electrodermal activity, respiratory patterns and cortisol levels. These biomarkers provide a more direct and quantifiable insight into the body's response to stress, making them valuable tools in stress assessment.

Experts specializing in research also meticulously design standardized questionnaires for the subjective evaluation of stress, which has been a longstanding approach to understanding individual stress levels. These questionnaires are structured to accurately capture an individual's perceived stress levels and their reactions to various stressors. This subjective methods are crucial as they offer insights into the personal experiences and perceptions of stress, which may not always be evident through objective measures.

2.2 Subjective Measures ^{‡MO}

Subjective ratings, such as self-report questionnaires, have been commonly used as a direct method to estimate levels of mental stress in humans in an experimental setting. (Aigrain et al. 2018). Participants are asked to answer a variety of questions about their experiences in the experiment. There have been a different variety of questionnaires and tests used to investigate the emotional state or perceived stress from the human participants in experimental setting. Some of the most widely used ones are Self-Assessment Manikin (SAM) (Bradley and Lang 1994), National Aeronautics Space Administration–Task Load Index (NASA-TLX) (Hart and Staveland 1988), Perceived Stress Scale (PSS) (Cohen, Kamarck, and Mermelstein 1983) etc.

The SAM is a non-verbal pictorial assessment technique designed to measure emotional response and affective reaction to diverse stimuli (Bradley and Lang 1994). Administered typically at the conclusion of each experimental task, it asks participants to assess their emotions and affective state on a scale from 1 to 9 across three dimensions: valence (the nature of the emotion, ranging from positive like relaxation to negative such as fear), arousal (the intensity of the emotion), and dominance (the extent to which the emotion is perceived as controllable).

NASA-TLX is extensively used in various research studies to evaluate mental stress levels. Notably, Nguyen and Zeng (2017) implemented this tool to assess the mental workload of surgeons during endoscopy training. In a similar vein, Zakeri et al. (2023) applied NASA-TLX within the context of smart factories to scrutinize factors like task complexity, time pressure, and collaboration duration, all contributing to mental stress.

Primarily, NASA-TLX aims to measure perceived workload across different tasks, particularly in high-stress environments. It seeks to capture a comprehensive picture of stress and workload through subjective user experiences. The tool does this by evaluating six key dimensions: Mental Demand, Physical Demand, Temporal Demand, Performance, Effort, and Frustration, each playing a role in the overall task load assessment for an individual. The evaluation process incorporates a NASA-developed technique for gauging the relative significance of these factors in the experienced workload. For each of the six dimensions, NASA-TLX employs a 21-point bipolar scale, allowing participants to range their workload assessment between two extremes, such as "Low/High." Furthermore, the process involves presenting pairs of rating scale labels, prompting subjects to choose which label is more pertinent to their cognitive workload experience in the task. This selection pattern enables the assignment of a weight to each cognitive load factor, culminating in an overall score that aligns with a specific subject's experience.

Nguyen and Zeng (2017) demonstrates the use of the NASA-TLX for assessing mental stress by interpreting workload measurements as indicators of stress levels. This approach highlights NASA-TLX's utility in evaluating how task demands can translate into mental stress.

In our research, NASA-TLX emerged as the most fitting tool for assessing stress in the context of the external stimuli of human-robot collaborative tasks. Stress, as a multifaceted experience, varies subjectively in perception. It might arise in response to workload (our focus area) but also encompasses factors such as emotional responses, individual coping mechanisms, and various personal and environmental influences. Characterized often by

feelings of strain, anxiety, or pressure, stress responds to both internal and external stimuli. Given our specific objective to assess stress related to the external stimuli of the task, other questionnaires like the Perceived Stress Scale (PSS), Trier Inventory for the Assessment of Chronic Stress (TICS) (Schulz and Schlotz 1999) - which measures general chronic stress over a period, or the Daily Stress Inventory (DSI) (Brantley et al. 1987) - evaluating daily stress events, did not align with our requirements.

While subjective questionnaire is a powerful tool to measure stress levels directly, it is important to mention their limitations. The reliance on self-reporting means it's subject to individual biases and may not accurately reflect real-time stress levels. People might not always be able to accurately introspect and report their feelings or may inadvertently skew their responses based on what they think researchers want to hear.

2.3 Objective Measures ^{†MO}

Objective measures of stress include measuring of physiological and physical measures by means of sensors. These sensors are either placed on the human body to measure bodily changes in an unobtrusive manner or at a distance in case of physical measurements. Objective measures of stress are free from human intervention and hence cannot be biased. The two sensors we used to collect biosignals objectively are the Empatica E4 and the OptiTrack Motion Capture System. They are introduced below:

2.3.1 Empatica E4

The Empatica E4 (Empatica n.d.[a]) (see Figure 2.1) wristband is a versatile and compact device designed to capture a wide range of physiological data in real time. It has four sensors: a Photoplethysmography (PPG) sensor, which measures Blood Volume Pressure (BVP); an EDA sensor, which is used for measuring GSR; a 3-axis Accelerometer to capture motion-based activity and an infrared thermopile to reads skin temperature (ST) (Garbarino et al. 2015). Its unobtrusive nature makes it comfortable to wear, while its comprehensive data collection capabilities have made it an invaluable asset.

The Empatica E4 wristband collects BVP data using the PPG with a process that involves emitting green and red light from LEDs into the skin and measuring the reflected light with a sensor(see Figure 2.2a). The green light, absorbed by the blood, provides a pulsatile signal corresponding to the cardiovascular pulse wave used to determine heartbeats. The red light acts as a reference to correct for motion artifacts. Algorithms then process this data within the wristband to output the BVP, from which the interbeat interval (IBI)—the time between heartbeats—is calculated, offering a non-invasive method to monitor heart rate continuously.(Empatica n.d.[c])

EDA is measured by detecting the electrical conductance across the skin, which is an indirect indicator of the sweat gland activity influenced by the sympathetic nervous system. To obtain these measurements, Empatica employs a method that relies on passing a minimal electrical current between two electrodes that are in contact with the skin, typically placed on the bottom wrist.

The wristband also includes a 3-axis accelerometer and an infrared thermopile, which can track body temperature and movement, providing a comprehensive overview of the

wearer's physiological state.



Figure 2.1: Empatica E4 features (Empatica n.d.[b])

Photoplethysmogram-PPG

Photoplethysmogram (PPG) also known as Blood Volume Pulse (BVP) are non-invasive optical techniques used to monitor changes in blood volume. They rely on the principles of light absorption and reflection to capture valuable information about cardiovascular activity. PPG sensors commonly found in wearable devices obtain BVP signals by transmitting light into the skin and measuring the amount of light either transmitted through or reflected back.(Roberts 1982)

When the heart beats, it propels blood through the circulatory system, causing periodic changes in the volume of blood vessels. PPG sensors emit light into the tissue and measure the amount of light that is either absorbed or reflected back. During each heartbeat, blood absorbs more light, leading to a decrease in the amount of light detected by the sensor. Between heartbeats, when blood flow is less pulsatile, more light is detected.(Zhang et al. 2001)

The resulting waveforms from PPG typically consist of a series of peaks and troughs, with each peak corresponding to a heartbeat (systole) and each trough representing the resting period between beats (diastole). By analyzing the time intervals between these peaks, the heart rate can be calculated. This heart rate measurement is fundamental and provides valuable information about a person's cardiovascular health and overall fitness level. It serves as a key metric in various applications, including exercise tracking, medical diagnosis and in our case here stress assessment.

Furthermore, PPG signals enable the assessment of HR and HRV. HRV is the variation in time between successive heartbeats and is an essential indicator of the autonomic nervous system's activity. By analyzing the subtle changes in the intervals between PPG peaks, HRV can be quantified. High HRV typically indicates a healthy heart and a well-balanced autonomic nervous system, while reduced HRV can be associated with stress, illness, or various medical conditions. HRV analysis provides insights into the body's ability to adapt

to different situations and is valuable for assessing stress levels, mental well-being, and overall cardiovascular health.

Other measures that can be derived from PPG data include and estimation of blood oxygen saturation levels (SpO_2), valuable for respiratory and circulatory health assessment. PPG can also be used to estimate respiration rate, reveal vasomotor activity changes associated with the autonomic nervous system, emotions, or vascular health, and provide insights into arterial stiffness and blood flow dynamics as well as blood pressure. First derivative and second derivate of PPG signals can also be analyzed. The first derivative (Velocity Plethysmogram, VPG) and the second derivative (Acceleration Plethysmogram, APG) features can be used for blood pressure estimation etc.(Suboh et al. 2022)

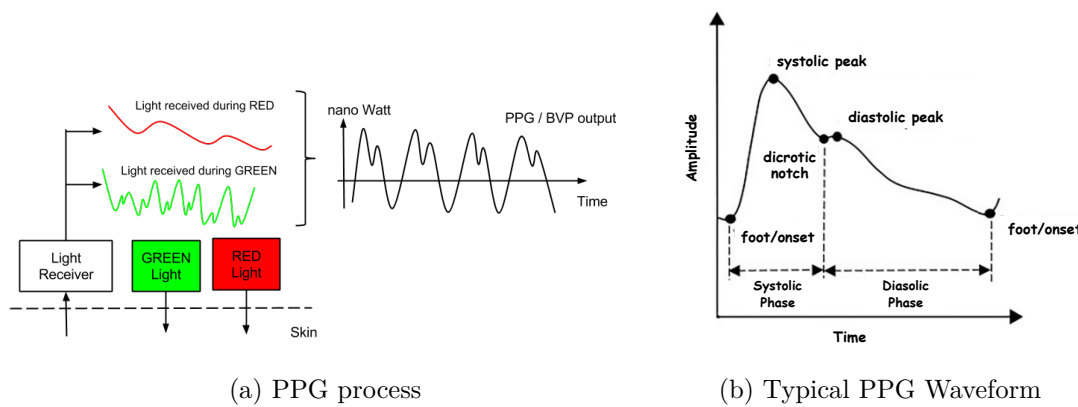


Figure 2.2: (Empatica n.d.[b]) (Suboh et al. 2022)

Electrodermal Activity-EDA ^{†MO}

Electrodermal Activity (EDA), also known as the galvanic skin response(GSR), is a way to measure changes in how our skin conducts electricity. Even moderate amounts of sweating that are not observable at the skin surface can alter skin electrical conductivity. The more the body sweats, the more conductive the skin becomes, and this change can be measured to infer physiological or psychological states. More specifically EDA measures the skin's electrical conductance changes, which depend on the quantity of sweat secreted by eccrine sweat glands in the hypodermis of the palmar and plantar regions. Sweat secreted in the palmar and plantar regions is caused mainly by central nervous activity related to affective and cognitive states, including mental or emotional sweating (Machado-Moreira et al. 2008). Thus, EDA becomes one of the promising noninvasive methods widely used in detecting stress and emotion. EDA is a powerful method for real-time measurement and could be used as an index of emotional or cognitive stimulation related to stress.(Gellman 2020). EDA is useful in several ways: it shows how we respond emotionally, helps us see how our body reacts to stress etc. It acts as a biomarker for emotional responsiveness and serves as a key indicator for stress-related bodily responses.

Electrodermal Activity (EDA) comprises two main components: the tonic and phasic components. The tonic component, also known as skin conductance level (SCL), reflects slow and consistent changes in the signal's background. In contrast, the phasic components, referred to as skin conductance response (SCR) or spontaneous fluctuation of skin response,

are the rapid and momentary fluctuations within the signal that occur within specific time intervals (2017). SCR appears in response to stimuli activating the sympathetic nervous system. Consequently, SCR can be linked to a stimulus and can be valuable in measuring cognitive stress levels. However, directly extracting the components of EDA isn't straightforward.

When EDA sensors measure skin conductivity (SC) signals, they typically yield results in microsiemens. To extract the SCL and SCR components accurately, it is necessary to deconvolve the SC signals (Alexander et al. 2005, postnote). Without proper separation of the original SC signals, overlapping SCRs can lead to less precise information during feature extraction . Therefore, it is crucial to perform deconvolution to distinguish the SCR and SCL signals effectively.

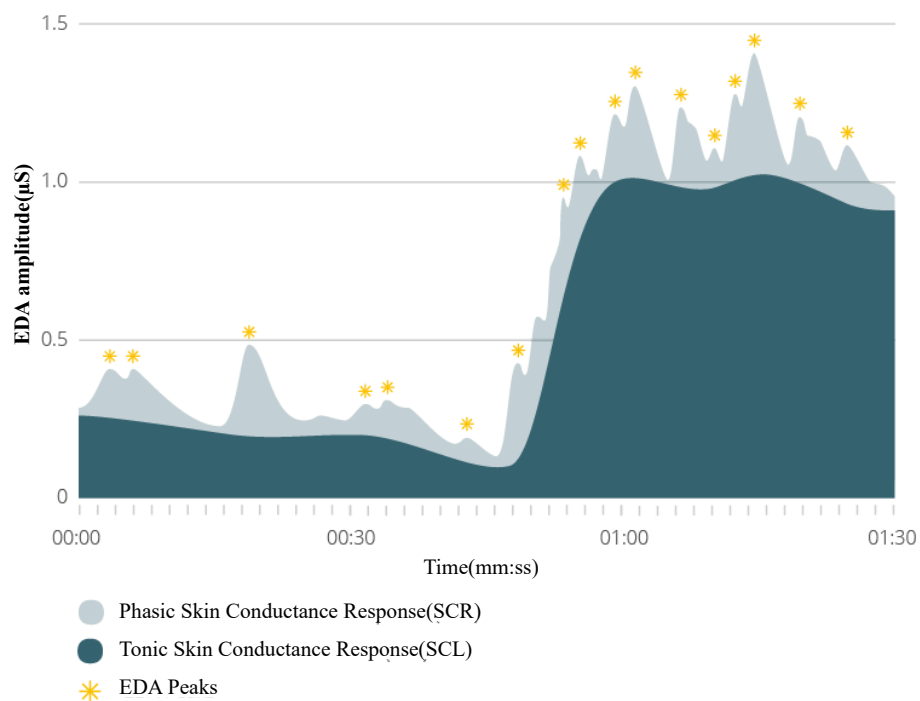


Figure 2.3: EDA Example signal - (imotions n.d.)

Skin Temperature

Other Physiological signal measured by the Empatica E4 is the skin temperature. Typically, the normal range for skin temperature lies between 33.5 and 36.9°C but changes in skin temperature can be connected to the stressful and anxious conditions (Empatica n.d.[c]) Skin temperature is strongly correlated to the heart activity and sweat reaction of an individual, so when a person is sweating, their skin temperature increases thus being a measure of increased stress levels.

2.3.2 Motion Capture

The OptiTrack Motion Capture System is a motion capture system that uses an array of 12 high-speed cameras equipped with advanced optics and infrared sensors. These cameras are positioned to cover a designated area, creating a three-dimensional space where every movement is tracked and recorded. The system detects reflective markers placed on key points of a subject's body. As the subject moves within the camera's field of view, the system tracks the spatial position and orientation of these markers, seamlessly translating physical movements into digital data.

For tracking the human body, the system uses a set of 25 marker points, which are placed at strategic points as shown in Figure 2.4. This configuration ensures a thorough capture of the upper body movements. The calibration process is a critical step where each marker on the subject's body is meticulously mapped onto a digital skeleton model. This mapping ensures that the system can accurately track the movements of each marker in relation to the body's overall structure. The system individually tracks each marker as the subject moves, allowing for a detailed representation of motion. The Motive software, integral to the OptiTrack system, plays a key role here. It enables users not only to visualize the movements in real time but also to record and analyze the data. The software translates the positional data of the markers into a skeletal animation, offering a clear and dynamic representation of the subject's movements.

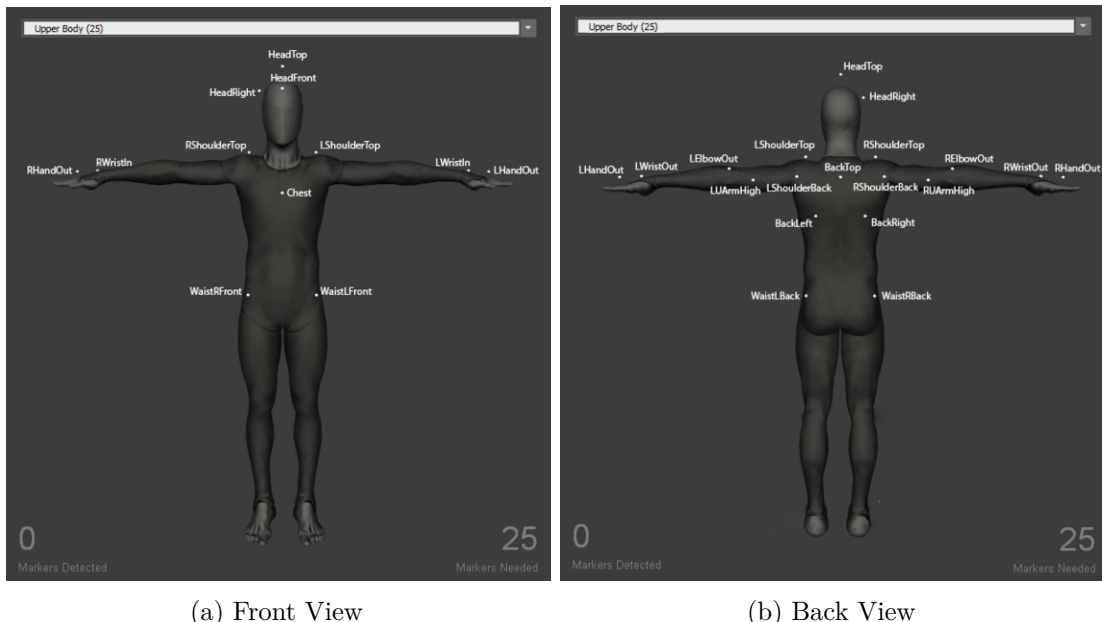


Figure 2.4: 25 Upper Body Marker Set (OptiTrack n.d.)

2.4 UR10 robot and Collision Avoidance ^{†MO}

The UR10 is part of the Universal Robots family of Collaborative Robots (Cobots), designed to collaborate directly with humans in a shared workspace. This robotic arm with six joints is highly flexible, has a reach of 1300 mm, and can handle a payload of up to

10 kg, making it suitable for a wide range of applications and collaborative tasks. Figure 2.8 shows the ur10 with its 6 rotatory joints.

Despite its capability to perform complex tasks, the UR10 does not inherently possess collision avoidance strategies. Its default response to encountering a collision is typically to halt operations to prevent any damage or injury, relying on built-in safety features that comply with industrial safety standards. However, innovative research and development have sought to enhance the UR10's capabilities with advanced collision avoidance strategies.

It is necessary to simplify the human body tracked using the motion capture system in ?? for ease of computation in collision avoidance trajectory planning. The simplified human body is modelled using line swept spheres (Larsen et al. 2000). A swept sphere, also known as a capsule, is the volume of a sphere that is swept along a straight line. It resembles a cylinder in shape, but it is simpler for distance metric computational purposes.

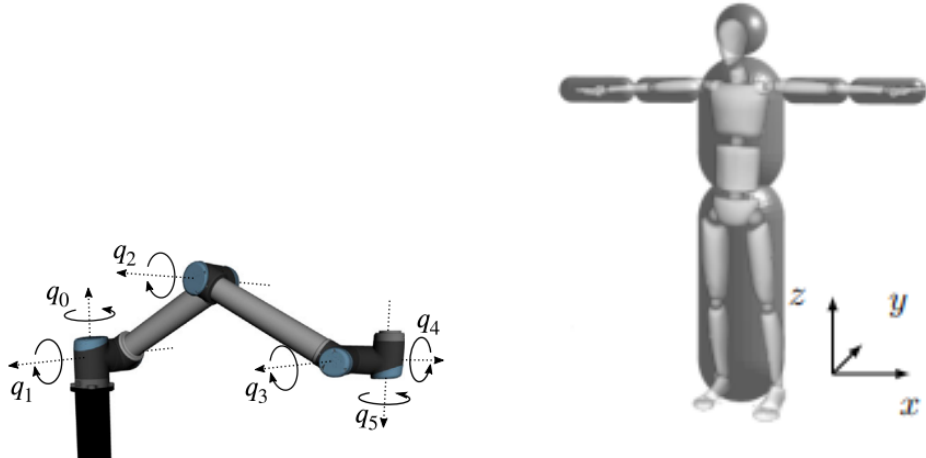


Figure 2.6: Simplified human model

Figure 2.5: 6 DOF UR10 taken from taken from (Renz, Krämer, and Krämer et al. 2020)

Bertram 2023a)

Seven spherical volumes make up the human body model: a sphere represents the head, while these swept sphere volumes represent the rest of the body parts, such as the arms, the torso and the parts below the hip is depicted by these swept spheres. This method effectively and precisely captures the human form and its movements in a simplistic manner, reducing complexity and increasing computational speeds. Figure 2.9 shows the simplified human body model superimposed on the skeleton model of the motion capture system. The motion capture system continuously monitors and records the individual's movements. This information is then fed into the robot's planning system, allowing it to maneuver and modify its actions adeptly in response to the human's changing position and movements.

This thesis discusses three different levels of collision strategies.

The first one already discussed is the default collision strategy of the UR10 robot, where it stops at a collision.

The second one uses dynamic collision avoidance, which tracks moving humans and tries

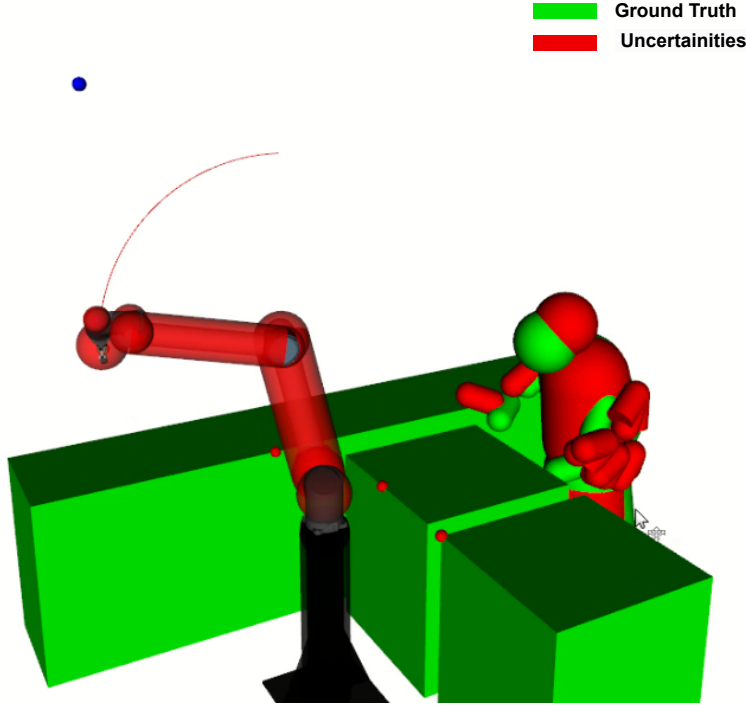


Figure 2.7: Predictive Collision Avoidance

to avoid them in real-time. It focuses Model Predictive Control (MPC), a method that anticipates and adapts to changes in the environment, including moving obstacles. This control scheme by Krämer et al. (2020) integrates online trajectory optimization with MPC. This approach enables the robot to adjust its movement in real-time, considering potential collisions and task variations. The prediction model within MPC approximates the robot's joint velocities and positions, facilitating efficient adaptation to dynamic obstacles. The control system is structured in a cascaded manner. The outer loop handles MPC, planning optimal movement trajectories, while the inner loop consists of tracking controllers for velocity references. This architecture effectively decouples the complex dynamics of robot motion control, simplifying the computational process.(Krämer et al. 2020)

The third predictive collision avoidance strategy is predicting the future human motion. One approach for predicting human motion is the extrapolation of the human skeleton's joint states in joint space using Polynomial Estimation (PE) methods as done by Renz, Krämer, and Bertram (2023a). This technique involves fitting a polynomial to past joint angles in a least-squares sense and predicting future joint states, which includes the joint angles and their velocities and accelerations. These predictions inherently come with some degree of uncertainty, especially as the prediction horizon extends further into the future. To represent this uncertainty, a Gaussian Mixture Model (GMM) is applied, which describes multiple potential future extrapolations. Each extrapolation is defined by observations of the errors between the predicted joint states and the actual (ground truth) joint states at different time steps. These errors are time-dependent, with the assumption that errors increase for predictions further into the future.(Renz, Krämer, and Bertram

2023b).

The GMM consists of several components, each representing a normal distribution with its own mean and covariance matrix. These components collectively form a probabilistic model of the potential errors in joint state predictions over time. The parameters of the GMM are updated using an Expectation-Maximization (EM) algorithm, which maximizes the likelihood of the observed data (the past prediction errors). However, due to computational constraints, the GMM is not updated with every new extrapolation but rather at set intervals considering the most recent set of extrapolations.

This GMM approach allows for the estimation of uncertainties in a real-time capable manner, which is crucial for adjusting the robot's motion plan to avoid collisions with humans dynamically and safely.

2.5 Stress Classification \ddagger_{MG}

The classification of stress levels in individuals has been the subject of extensive research, leading to the development of various methods. Stress classification is a supervised learning problem, a category of machine learning. In supervised learning, the model is trained on a labelled dataset, meaning each input data point is associated with a known output label. In the context of stress classification, these labels represent different stress states, such as 'stressed' or 'not stressed'. The model learns from this training data, enabling it to make predictions or classify new, unseen data based on recognised patterns.

Among the various techniques employed for stress classification, Support Vector Machines (SVM), K-nearest neighbors (KNN), Logistic Regression, and Decision Trees are notable for their widespread use. These methods each have unique foundational concepts and operational mechanisms:

- **Support Vector Machines (SVM):** SVMs are known for their efficacy in classifying non-linearly separable data. They function by identifying the optimal hyperplane that separates different classes in the feature space.
- **K-Nearest Neighbors (KNN):** KNN classifies data based on the similarity principle, considering how closely a new data point resembles existing points in the training set. This method is particularly useful when dealing with irregular decision boundaries.
- **Logistic Regression:** Commonly used for binary classification, Logistic Regression computes the probability that a given input belongs to a particular class, ideal for cases where the output is a probability or a binary decision.
- **Decision Trees:** Decision Trees employ a tree-like model of decisions, where each node represents a feature, each branch represents a decision rule, and each leaf represents an outcome. They are simple to understand and interpret and are useful for both classification and regression tasks.

Research by Bhushan and Maji (2023), Gedam and Paul (2021), Vos et al. (2023), and Sharma and Gedeon (2012) has been instrumental in reviewing, summarizing, and

comparing these commonly utilized methods in stress classification. Their analyses provide insights into the efficiency, applicability, and specificities of these classifiers, offering a deeper understanding of their role in stress level classification. This section aims to present an overview of the background information of these chosen classifiers.

Support Vector Machine

Support Vector Machine (SVM) is a supervised machine learning algorithm widely used for classification and regression tasks. At its core, SVM aims to find the optimal hyperplane that separates data points of different classes in a high-dimensional space. This separation is achieved to maximise the margin between the data points of other classes, ensuring the best possible classification.

The process of selecting the best hyperplane for data separation follows a methodical approach, adaptable for both binary and multiclass scenarios. Here's a general overview of the steps involved:

To separate data points into distinct classes, SVM employs kernel functions, which can be denoted as $K(\mathbf{x}_i, \mathbf{x}_j)$. These kernel functions transform the input data into a higher-dimensional space where a hyperplane can be used for separation.

The support vectors are the data points closest to the hyperplane and satisfy the following conditions:

$$\mathbf{w} \cdot \mathbf{x}_+ + b = +1, \quad \text{for positively labeled data,} \quad (2.5.1)$$

$$\mathbf{w} \cdot \mathbf{x}_- + b = -1, \quad \text{for negatively labeled data.} \quad (2.5.2)$$

These points are vectors \mathbf{x}_+ and \mathbf{x}_- that lie on the boundary of the margin.

The margin is defined as the distance between the support vectors and the hyperplane. It can be calculated as:

$$\text{margin} = \frac{2}{\|\mathbf{w}\|}. \quad (2.5.3)$$

The optimal hyperplane is the one that maximizes the margin. The objective function to maximize the margin while classifying the training data correctly is given by:

$$\max_{\mathbf{w}, b} \frac{2}{\|\mathbf{w}\|}, \quad \text{s.t. } y_i(\mathbf{w} \cdot \mathbf{x}_i + b) \geq 1, \quad \forall i. \quad (2.5.4)$$

This can also be equivalently written as a minimization problem:

$$\min_{\mathbf{w}, b} \frac{1}{2} \|\mathbf{w}\|^2, \quad \text{s.t. } y_i(\mathbf{w} \cdot \mathbf{x}_i + b) \geq 1, \quad \forall i. \quad (2.5.5)$$

By solving this optimization problem, SVM finds the optimal hyperplane that classifies the data with the maximum margin, enhancing the generalization ability of the classifier. The SVM stands out from other classifiers that also use lines or hyperplanes due to its strategy of utilizing the maximum margin separating hyperplanes. By focusing on this maximum margin, the SVM enhances its ability to correctly predict the classification of new, previously unseen instances. The chosen hyperplane effectively determines how an unknown sample is classified, falling into one class or another based on which side of the hyperplane it lies. This approach ensures that the classifier is not only effective but also

robust in its predictions, making SVM a valuable tool in a wide range of classification applications.

Support Vector Machines (SVMs) are particularly well-suited for the task of stress classification from physiological data. By constructing an optimal hyperplane in a high-dimensional feature space, SVMs can efficiently differentiate between stressed and non-stressed states based on various biosignals. The mathematical foundation of SVM in the context of stress classification can be represented as follows:

Below is the table of common kernel functions used in SVM:

Table 2.1: Kernels

Kernel	Expression
Linear Kernel	$K(\mathbf{x}_i, \mathbf{x}_j) = \mathbf{x}_i^\top \mathbf{x}_j$
Polynomial Kernel	$K(\mathbf{x}_i, \mathbf{x}_j) = (\mathbf{x}_i^\top \mathbf{x}_j + c)^d$
Sigmoid Kernel	$K(\mathbf{x}_i, \mathbf{x}_j) = \tanh(\beta \mathbf{x}_i^\top \mathbf{x}_j + \theta)$
RBF	$K(\mathbf{x}_i, \mathbf{x}_j) = \exp(-\gamma \ \mathbf{x}_i - \mathbf{x}_j\ ^2)$

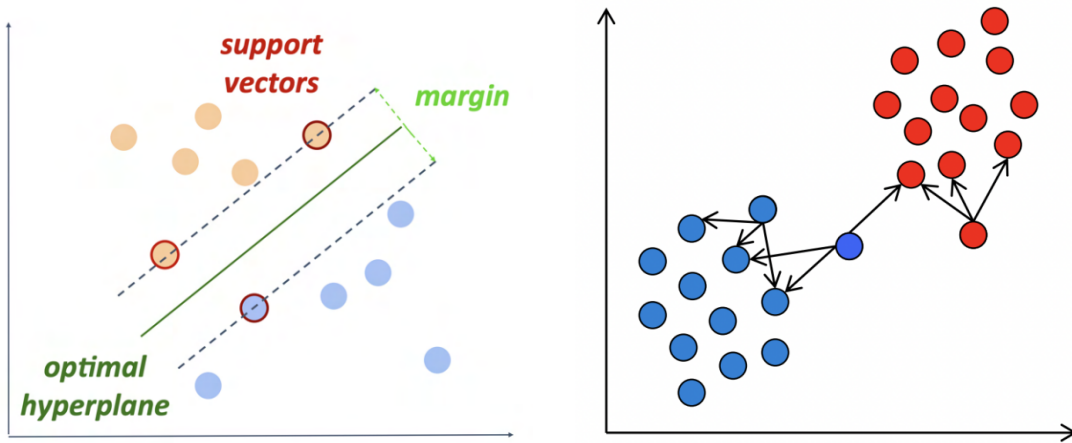


Figure 2.8: SVM taken from (Badillo et al. 2020)
Figure 2.9: kNN taken from (Badillo et al. 2020)

K-Nearest Neighbors (KNN)

K-Nearest Neighbors (KNN) is a versatile algorithm used in supervised machine learning, predominantly employed for classification and, to some extent, regression tasks. It operates on the principle of classifying new data points based on the majority class among its nearest neighbors in the feature space. The proximity of neighbors is determined using distance metrics, such as the Euclidean distance and Manhattan distance, calculated by the following formulas:

$$\text{Euclidean Distance}(\mathbf{x}_i, \mathbf{x}_j) = \sqrt{\sum_{k=1}^n (x_{ik} - x_{jk})^2} \quad (2.5.6)$$

$$\text{Manhattan Distance}(\mathbf{x}_i, \mathbf{x}_j) = \sum_{k=1}^n |x_{ik} - x_{jk}| \quad (2.5.7)$$

The choice of ‘ k ’, the number of nearest neighbors to consider, is critical. A smaller ‘ k ’ can make the model sensitive to noise, while a larger ‘ k ’ can lead to high computational costs and may include less relevant neighbors. Optimal ‘ k ’ is often determined through cross-validation.

Some variations of KNN employ weighted voting, where closer neighbors have more influence on the classification than more distant ones, enhancing the accuracy in certain scenarios.

KNN is effective for stress classification in datasets where stress indicators form distinct clusters. In physiological data, for instance, patterns of stress responses might cluster, enabling KNN to differentiate between stressed and non-stressed states. While KNN’s simplicity and effectiveness are advantageous for smaller datasets, it faces challenges like high computational cost in large datasets and sensitivity to irrelevant features. Feature selection and dimensionality reduction techniques are employed to mitigate these issues. In conclusion, KNN’s approach of classifying data based on nearest neighbors, along with its adaptability to distance metrics like Euclidean and Manhattan distances, makes it a valuable tool for stress classification. Key considerations for its effective application include dataset size, feature relevance, and the optimal choice of ‘ k ’.

Logistic Regression

Logistic Regression is a widely-used statistical method in supervised machine learning, particularly suited for binary classification tasks. It predicts the probability of a certain class or event based on one or more independent variables, making it ideal for outcomes that are categorical, such as ‘yes/no’, ‘true/false’, or ‘stressed/not stressed’. The fundamental concept of Logistic Regression is to estimate the probabilities of different possible outcomes of a categorically distributed dependent variable, given a set of independent variables. This is achieved using the logistic function, an S-shaped curve that can map any real-valued number to a value between 0 and 1. The logistic function, also known as the sigmoid function, is central to Logistic Regression and is defined as:

$$\text{Sigmoid}(\theta) = \frac{1}{1 + e^{-\theta}} \quad (2.5.8)$$

Here, θ represents the linear combination of the input features. The model expresses the probability that each input belongs to a certain class as a function of this logistic function. Logistic Regression is particularly effective for binary classification tasks, such as stress classification. It models the probability that a given input is ‘stressed’. The model outputs a probability score, and a threshold, usually set at 0.5, is used to classify the input into one of two classes.

While traditionally used for binary classification, Logistic Regression can be extended to multi-class classification problems, such as classifying inputs into three distinct classes. Techniques like One-vs-Rest (OvR) and Multinomial Logistic Regression allow for handling

multiple classes. The Softmax function is often employed in these cases to generalize the Logistic Regression model for multiple classes.

Logistic Regression is valued for its simplicity and interpretability, requiring low computational resources. It assumes a linear relationship between the independent variables and the logit of the dependent variable, and may not perform well with complex relationships in data, where methods like SVM or Neural Networks could be more suitable. In conclusion, Logistic Regression's probabilistic outputs and straightforward implementation make it a popular choice for binary classification tasks, including stress level classification, and its adaptability to multi-class classification further enhances its utility in various applications.

3

Data Collection-Subject Study

A collaborative assembly task involving wooden pieces was designed in the robot laboratory of the Institute of Control Theory and Systems Engineering at the Technical University of Dortmund. This setup aims to accurately replicate tasks commonly seen in industrial settings where collaboration between humans and cobots is frequently observed. The Universal Robot UR10 was selected as the cobot to be used in the study. A call for participants invite was sent out, and 20 male students who all had a technical background volunteered to participate in the study. Seventeen of the students did not have any previous experience working with a robot in any way, whereas the remaining had some previous experience with robots. All of them were between the ages of 21 and 28. Before the experiment began, all participants were given a comprehensive overview of the study's objectives and procedures, along with a consent form. Only those participants who agreed to the terms and signed the consent form were permitted to proceed with the experiment. To ensure the ethical integrity of the study, a prior request for ethical approval was submitted to the appropriate ethics council and permission was obtained to conduct the subject study.

3.1 Design of Tasks

For the purpose of studying the impact of stress on various factors, the assembly of different mock items using wooden children's toys was chosen as a method of replicating an industrial assembly task.

These included three distinct levels of different collaboration levels:

- **Separated Worksapce:** Human and cobot have no overlapping workspace. The cobot works in the background. The human already has all items required for the assembly task in front of him.
- **Shared Workspace:** The human and cobot share the same work area. The cobot brings each item required for the assembly tasks to the human and places it on the table in front of the human.
- **Shared Workspace with Direct Collaboration:** The human and cobot share the same work area and the cobot brings the item required for the assembly tasks to the human and directly hands over the items to the human.

Collision Avoidance Strategy	Separated Workspace (A)	Shared Workspace (B)	Shared Workspace with Direct Collaboration (C)
No Collision Avoidance (X)	AX	BX	CX
Dynamic Collision Avoidance (Y)	Not Required	BY	CY
Predictive Collision Avoidance (Z)	Not Required	BZ	CZ

Table 3.1: Task names for different Collision Avoidance Strategies and Workspace Scenarios

As well as three robot collision avoidance strategies:

- **No Collision Avoidance:** No collision avoidance measures are in place, and the robot stops at a collision.
- **Dynamic Collision Avoidance:** The robot identifies the human as a dynamic obstacle and adjusts its trajectory to avoid collisions.
- **Predictive Collision Avoidance:** This strategy uses predictions to predict the human's future position and adjusts its trajectory to avoid collisions.

The Table 3.1 shows the various combinations of factors and the naming conventions of the tasks, yielding seven experimental scenarios since collision avoidance is not applicable when Separated Workspaces are involved. For example, task BZ employed a predictive collision avoidance strategy while doing the task in a shared workspace. So a within-subject experimental design was employed where each participant was tested on all seven scenarios. By having the same participants perform each task, we minimized the impact of differing skill sets, experiences, and cognitive abilities, which could otherwise skew the results.

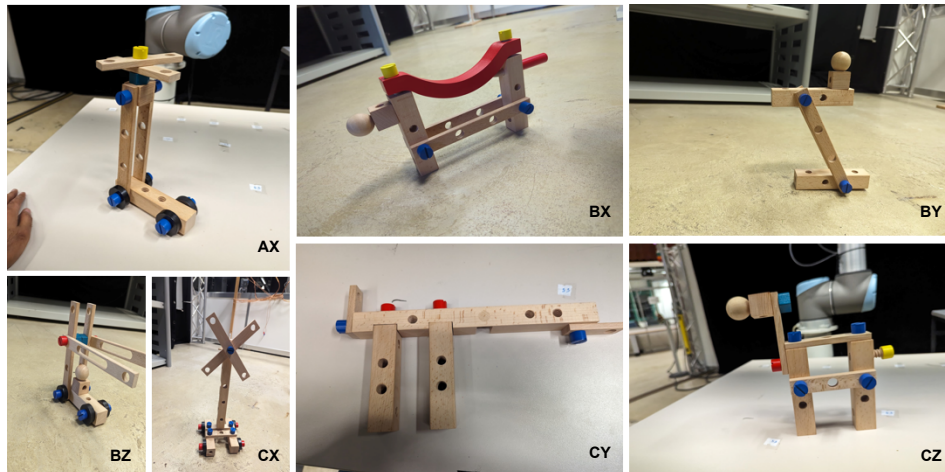


Figure 3.1: 7 different assembly tasks

To avoid any potential learning effects and ensure that each task measures the intended variables accurately, we had to design seven different assembly tasks. Each task involved assembling a unique item, chosen of similar complexity and required effort. This similarity in task difficulty was crucial to avoid the introduction of other variables, such as familiarity with the task, which could affect the results. Figure 3.1 shows the final assemblies completed in each of the seven tasks. Each task had approximately 4-6 different parts, which were supposed to be screwed together to complete the tasks. By standardizing the complexity across tasks, we aimed to isolate the impact of the collision avoidance strategies and collaboration levels. We also had to consider the order in which the task was administered for each participant, ensuring that learning or fatigue does not affect the outcomes in any way. Each participant experienced the tasks in a unique order, balancing out any potential biases introduced by the order of task presentation.

3.2 Apparatus and Experimental Setup

The experiment was set up in a specially designated area of our laboratory. Figure 3.2 shows the experimental setup. At the center of this arrangement was the collaborative workspace, featuring a table and chairs for the human participant (Area B in Figure 3.2), positioned directly opposite the robot's dedicated workspace. Adjacent to this, on the right side of the collaborative workspace, a table was placed to hold the various items needed for the assembly tasks (Area A Figure 3.2). The robot would pick the necessary items from this table for each specific task and deliver them to the human participant. In front of the human participant, a mobile device was also placed. This device was key to the experiment, as it presented the participant with concise, step-by-step instructions for each assembly task. Figure 3.5a shows how these instructions were visually displayed, offering clear and easy-to-follow guidance. The participant would start the assembly task as soon as the first item is delivered to the human participant. The robot would then proceed to the next item, and so on until all items are delivered to the human participant.

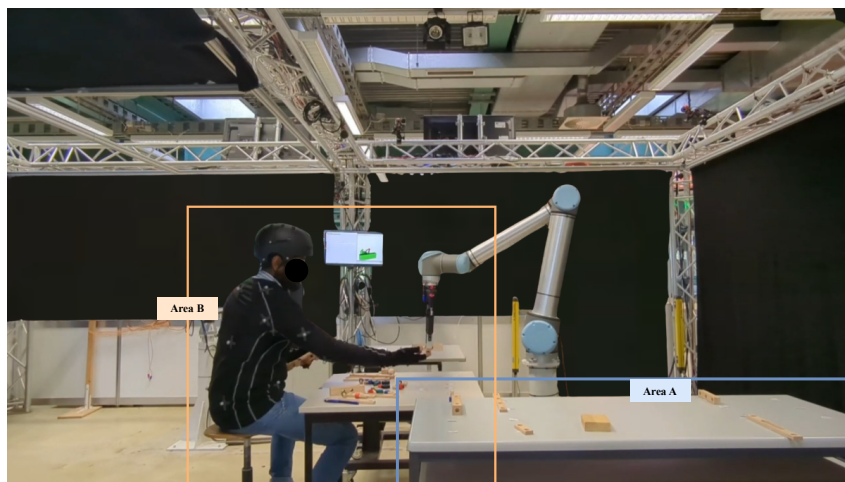


Figure 3.2: The experimental setup

The entire experimental area had an OptiTrack motion capture system, outfitted with 12 high-precision cameras fitted across all 4 sides as partly seen in Figure 3.3. These

OptiTrack cameras, known for their accuracy and low latency are used to capture every detail of the human participant's movements. This setup was necessary for the collision avoidance trajectory planning for the robot and also providing a detailed and continuous record of the participant's interactions with the robot. The use of the OptiTrack system enabled us to gather precise data on human motion. The participants were equipped with the motion capture suit which had 25 distinct marker points which were used to capture the human's head and upper body. To prioritize participant safety, especially given the proximity to a large robotic arm, a helmet also equipped with the head markers was provided to each participant.

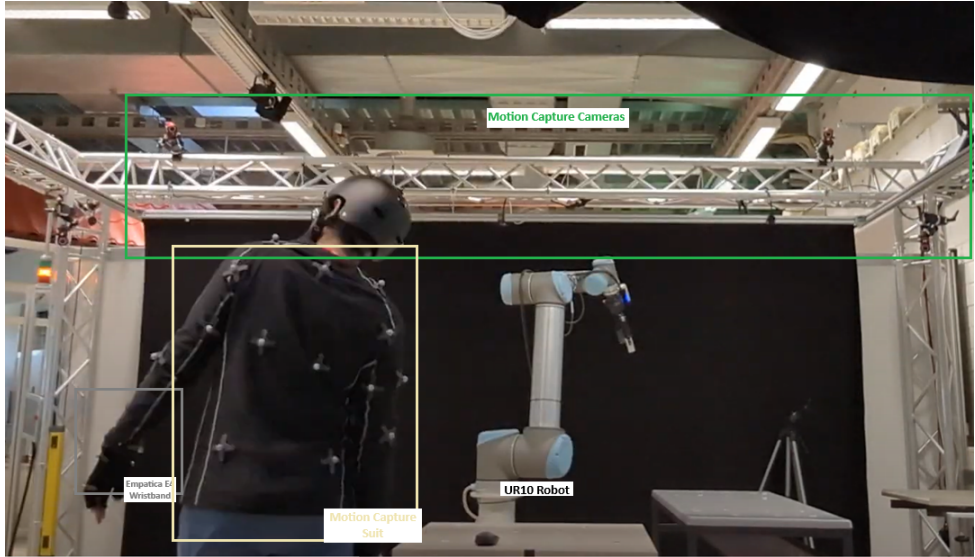


Figure 3.3: Apparatus used

For capturing the physiological signal of the participants, the Empatica E4 wristband was equipped on the participant's non-dominant hand. The participant's physiological signals such as GSR, EDA, HR and temperature, are captured by the Empatica E4 wristband, which transmits data wirelessly via Bluetooth to a Windows PC. This PC with an Intel i5-12600KF at 3.7 GHz using 32 GB RAM and a NVIDIA GeForce RTX 3060 with 12 GB VRAM. runs the E4 streaming server as well, facilitating the real-time transfer of this data. The various motion capture cameras recording the participant's movements are synced together and are connected to the Windows PC as well running the motion capture software, Motive. The physiological data from the Empatica E4 and the motion data from the motion capture system are then streamed to a Linux PC running the Robot Operating System (ROS)1 Melodic. The motion capture data is published to `/tf` topic. Whereas the Empatica E4 node is available as a ROS2 node running inside a docker container interfacing with the ROS1 using a ROS bridge. Then a data synchronization script is used to create a ROS node that subscribes to the multiple topics from various sources, synchronizes the incoming data, and publishes a compiled message to the `/aggregated_data` topic. A more detailed description of the data synchronization process is provided in section 4.1. This synchronized data topic is then recorded to a rosbag. A general schematic of this is shown in Figure 4.1.

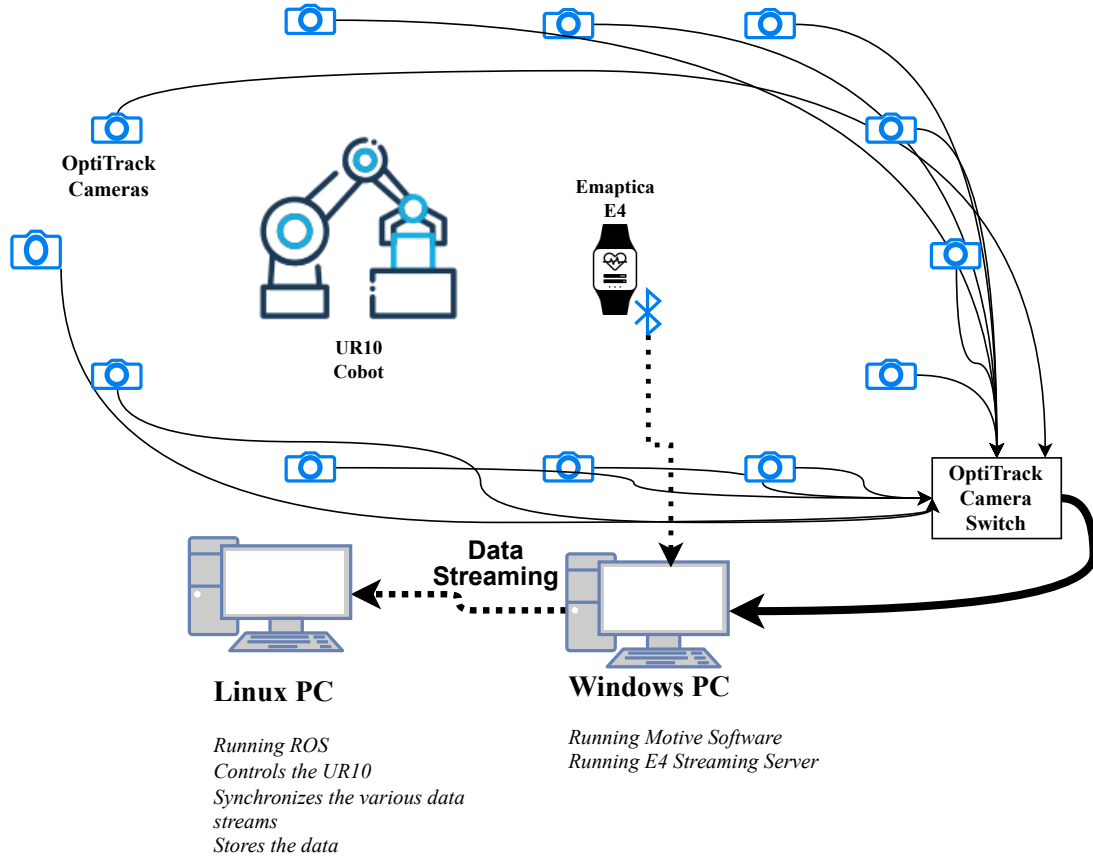


Figure 3.4: Schematic of the experiment setup

3.3 Experimental Procedure

The participants visited the experiment room in the time slot they had selected. Upon arrival, they were greeted and guided through a comprehensive orientation that explained the experimental procedures. This session included detailed descriptions of the various equipment involved, such as the Empatica E4 wristband for monitoring physiological responses and the motion capture system for observing and recording precise movement. Each participant was fitted with the motion capture suit and the Empatica E4 wristband, which was placed on their non-dominant hand, and both were carefully calibrated for accurate data collection.

Participants then were given an initial questionnaire that included a consent form, general information, and questions about their prior experience with cobots as well as the General Attitudes Towards Robots Scale (GAToRS) questionnaire (Koverola et al. 2022).

Once the preliminary documentation was complete, we established a baseline of physiological signals for each participant, which involved recording data for 2 minutes without any interaction with the cobot. This step ensured that we had a standard reference point for each participant's physiological state prior to beginning the tasks.

The main experimental procedure involved a sequence of seven distinct tasks, with the sequence randomized for each participant to control for learning effects. Before the start of each task, a two-minute briefing was provided. This briefing not only outlined the objec-

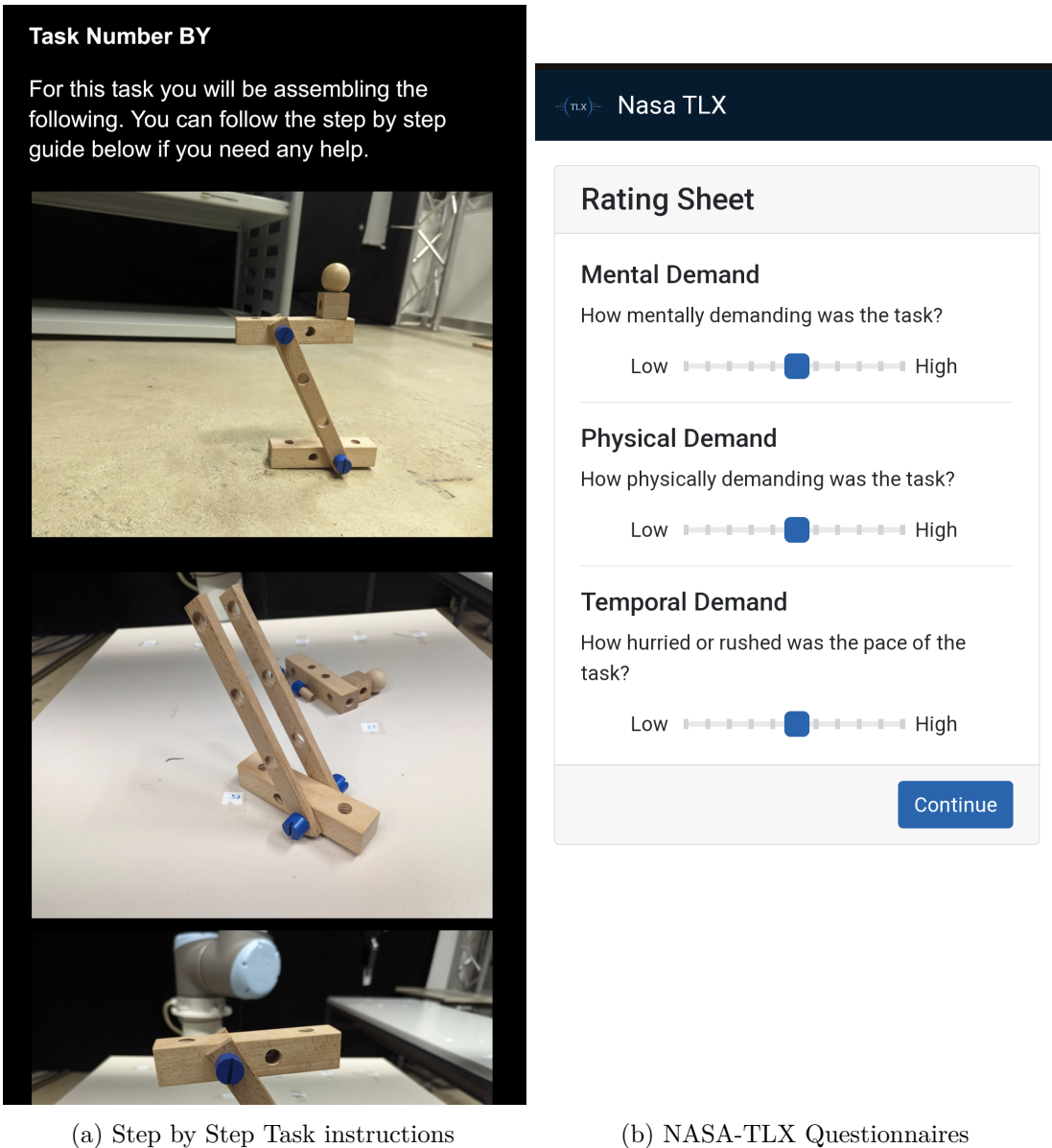


Figure 3.5: Screenshots from mobile device

tives and requirements of the task but also walked the participant through the instructions displayed on a mobile device, ensuring clarity and preparedness. Figure 3.5 illustrates the interface that participants encounter on the mobile device during the experiment. After the introduction, participants performed the task (Task i), during which both physiological and motion data were recorded. Each task lasted for about 5 minutes in average.

Upon completion of each task, participants were asked to fill out a post-task questionnaire. This included the NASA-TLX (as a webapp by Pandian and Suleri (2020)) to assess cognitive workload and the SAM to measure emotional response. These instruments were crucial for evaluating the impact of the task on the participant and infer subjective stress levels and emotional well-being from each task. Whilst the participants were filling the questionnaires, the experimental setting was reset to their original position in preparation for the next task.

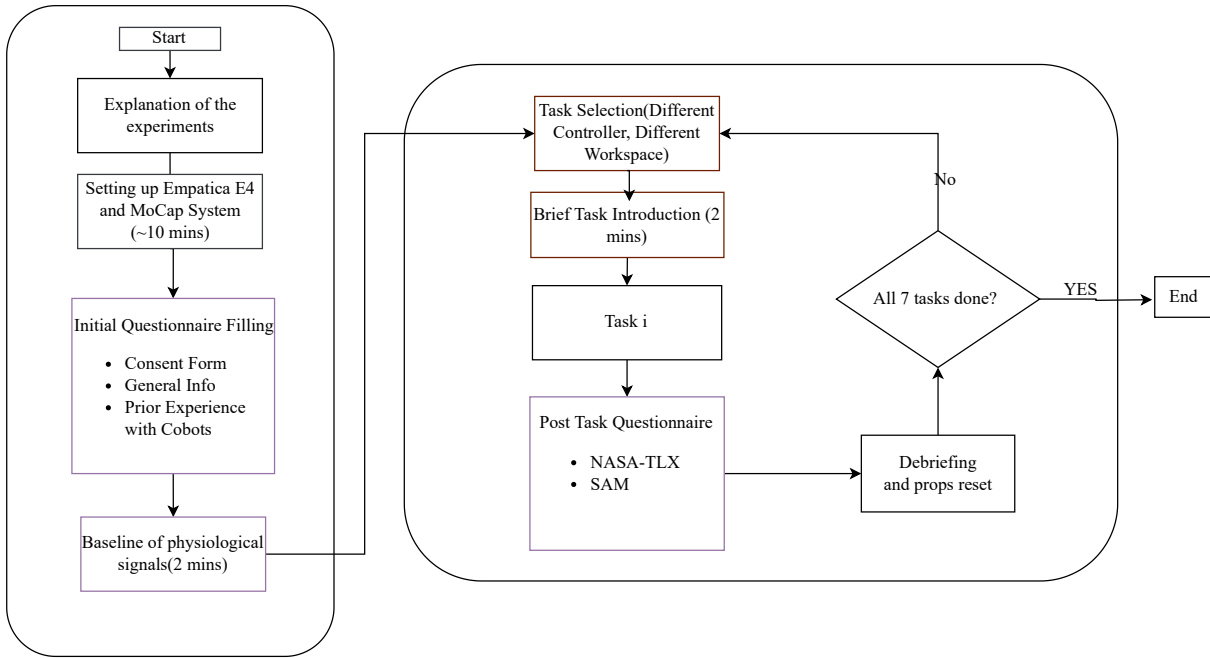


Figure 3.6: Schematic of the experiment protocol

After a participant had completed all tasks, we conducted a debriefing session. During this session, the participant could provide feedback and discuss their experiences as well explain the whole aim of the study and research. The whole session lasted for 45-60 mins on average

The structured design of this protocol ensured the collection of consistent and reliable data on human-robot interaction, with careful consideration of participant engagement and task impact.

4

Stress Detection Methodology

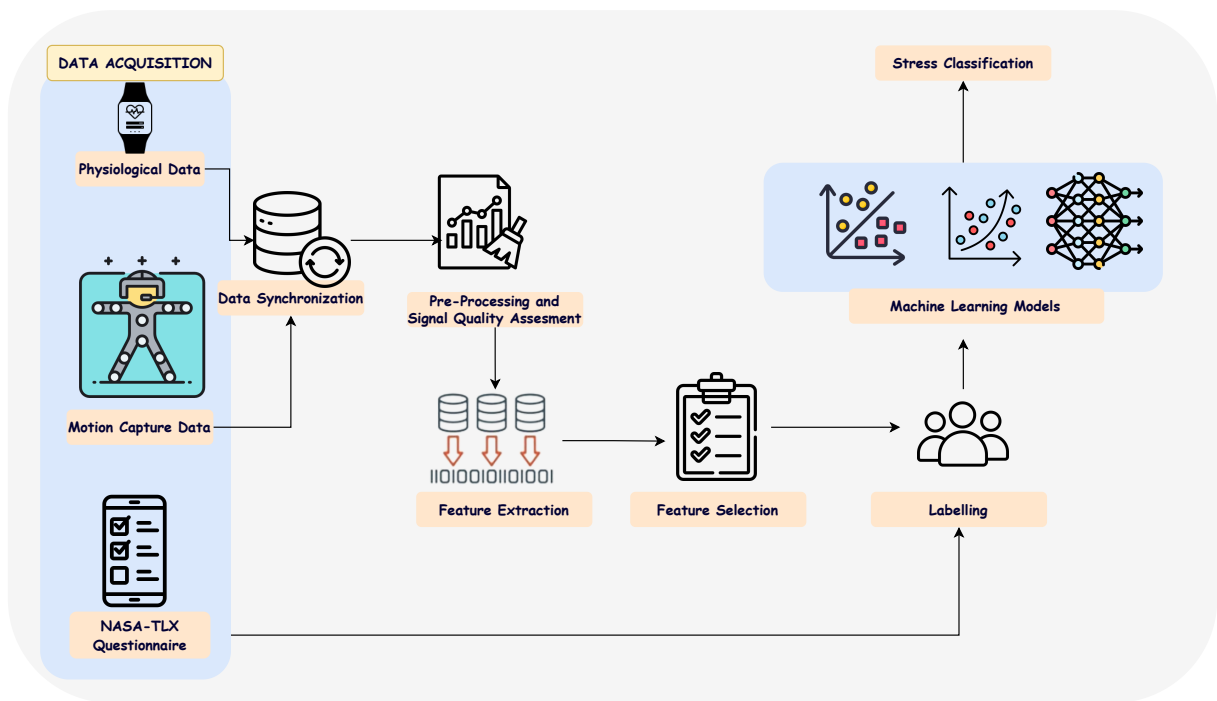


Figure 4.1: Schematic of the experiment setup

4.1 Data Synchronization^{†MO}

As previously eluded in section 3.2, data synchronization is crucial to our experimental framework, ensuring the consistency of data gathered from all the different sensors. In our setup, the Empatica E4 wristband collects various physiological signals, such as the Blood Volume Pulse(BVP), Electrodermal Activity (EDA), Heart Rate (HR), and Skin Temperature(ST) at different frequencies, as well as the motion capture system that tracks the participant's movements at a higher frequency. Given the varying sampling rates of these data sources, it's crucial to synchronize them to ensure they are comparable and accurate.

The Empatica E4 samples the Blood Volume Pulse (BVP) data at a rate of 64Hz. However, it transmits other metrics like EDA and temperature at a lower rate of 4Hz. On the other hand, the Motive software captures the motion capture data at a higher rate of around 120Hz. These differences in sampling rates require a careful synchronization approach. Our synchronization strategy focuses on aligning all the different data streams to uniform and matching frequency. Considering the need for detailed data where we retain most of the information required, we standardize all data streams to a frequency of 64Hz, matching the Blood Volume Pulse (BVP) rate from the Empatica E4. This standardization process involves downsampling the motion capture data, originally recorded at a higher frequency of 120Hz. Simultaneously, for other signals like the Electrodermal Activity (EDA) and temperature, updating at a lower frequency of 4Hz, and acceleration data at 32Hz, we use a forward-filling approach, carrying their most recent values until an update occurs.

A specialized ROS node is responsible for this synchronization. By using the BVP rate as the master reference, the node ensures that both physiological and motion data are synchronized in time. This alignment is critical for an integrated and comprehensive analysis of the participant's responses, providing a dataset that accurately reflects both the physiological states and motion data.

Once synchronized, the data is then published to a ROS topic, typically */aggregated_data*. This topic carries a comprehensive stream of information that combines detailed physiological measures with motion data. This dataset forms the foundation for subsequent analysis phases in our study, such as feature extraction and stress detection.

4.2 Pre-Processing^{†MO}

Pre-processing is a crucial step in analysing data from physiological sensors and motion capture systems, as it prepares the raw data for subsequent processing and analysis phases. This section outlines the key aspects of pre-processing in our study.

Data Filtering

In the pre-processing phase of our study, data filtering plays a crucial role in refining the quality of the signals gathered from the physiological sensors and motion capture systems. This step involves applying specific filtering techniques to the raw data to remove unwanted data, thereby enhancing the signal's clarity and usability for further analysis.

The primary objective of data filtering is to isolate the significant aspects of the signal while eliminating any unwanted noise or interference. Different filtering methods are employed depending on the nature of the signal and the type of noise present. For instance, we use N-th-order Butterworth filters, which effectively retain the desired frequency range while attenuating frequencies outside this range. The Butterworth filter is known for its smooth frequency response and is particularly useful in physiological signal processing, where preserving the signal's integrity is crucial.

Each signal type dictates specific filter parameters like filter order, cutoff frequencies, and filter type (lowpass, highpass, or bandpass). This careful selection ensures that the final signal is representative of the true physiological data crucial for accurate analysis.

Data Normalization

Normalisation is a critical step in data pre-processing as well, particularly when dealing with signals of varying magnitudes or scales. Our approach involves applying a normalisation process to each input signal, standardising the data values range. This step is essential for comparing and combining data from different sensors effectively.

The method we use for normalisation is primarily the 'z-score' method. This technique transforms the data into a mean of zero and a standard deviation of one. Doing so ensures that each signal contributes equally to the analysis, irrespective of their original scale or distribution. This standardisation is crucial for machine learning models, as it enhances algorithm performance and prevents any single feature from dominating due to its scale. Normalisation also aids in mitigating the impact of outliers, as it brings all data points onto a common scale, making them more suitable for analysis.

Signal Quality Assessment^{‡MO}

Signal quality assessment is an integral part of the preprocessing phase to ensure the reliability and accuracy of data collected from sensors, which is fundamental for accurate analysis. Various methods are employed to assess the quality of signals, each targeting specific types of anomalies or artefacts.

Detection of Clipped Segments: This method involves identifying segments in the signal that are clipped or truncated. Clipping often occurs when the signal amplitude reaches the sensor's recording capacity limits. By setting thresholds for positive and negative clipping, the method detects and marks these segments, facilitating their exclusion or correction.

Detection of Flatline Segments: This method identifies flatline segments where the signal shows minimal variation over a period. Such segments can indicate sensor displacement or malfunction. The method identifies these periods by assessing the duration of flatness and the threshold for change in signal amplitude, helping exclude non-physiological data from the analysis.

Each method plays a crucial role in verifying the integrity of the signal data. Identifying and addressing issues like clipping, flat-lining, and inconsistent patterns, signal quality assessment ensures that subsequent data analysis stages are based on accurate and reliable data.

Baseline Correction

Baseline correction forms a pivotal part of our data normalization strategy, particularly tailored for participant-specific physiological data. This approach is centered around the concept of adjusting the data relative to each participant's baseline physiological state, captured during a rest period prior to the experimental tasks. This preparatory measure establishes a reference point against which subsequent physiological responses are compared. In the baseline correction process, we begin by computing the average values of physiological signals recorded during the baseline phase before the start of the experiment.

This baseline phase is critical as it represents a period of rest where the participant's physiological state is unaffected by experimental stressors. By establishing this baseline, we are able to set a reference point that reflects the participant's normal physiological state. Subsequently, we adjust the data points collected during the active phases of the experiment relative to these baseline averages. This adjustment is a normalization process that centers the data around a personalized zero point, effectively accounting for individual physiological variations. The core advantage of baseline correction lies in its ability to mitigate the influence of inter-individual variability on the physiological measurements. Since each participant exhibits unique baseline characteristics and responds differently to stressors and other factors, the process of normalizing data against individual baselines serves as a valuable means to address this variability and achieve a more accurate and personalized assessment of stress responses.

This method ensures that the changes observed in the physiological data during the experiment are indicative of the participant's response to the experimental conditions rather than being a reflection of their baseline physiological state.

Signal Segmentation

In our research, the segmentation of physiological data into windows was a crucial part of the preprocessing. This process involved breaking down the continuous data streams into smaller, manageable windows for detailed analysis. The selection of window size and step size was critical and was tailored based on the characteristics of the signal and the objectives of our analysis.

The window size was carefully chosen to capture relevant physiological and behavioral patterns within each segment, balancing the need to encapsulate meaningful data against the computational demands of processing. The step size determined the overlap between these windows, ensuring continuity and that no significant transient events were missed. Accounting for the sampling rate of each signal was vital in customizing the segmentation process appropriately. This flexible approach was key to accommodating different types of signals, ensuring that the window size was appropriate for the length of the signal and that the segmentation parameters were compatible with each signal's nature.

Segmenting data into Windows enabled us to convert the ongoing data streams into a format suitable for comprehensive analysis. This structured approach facilitated subsequent computational processes, including feature extraction and pattern recognition, essential for robust stress detection and analysis. This method of using windows in data segmentation is fundamental in ensuring that each part of the continuous data stream is analyzed effectively, allowing for a thorough understanding of stress indicators within the dataset.

4.3 Feature Extraction ^{†MO}

Feature Extraction and Selection play a pivotal role in the effectiveness of machine learning models, especially in the context of human stress recognition. Feature extraction involves deriving meaningful attributes from the raw data collected. The features extracted can vary widely, including statistical features, time-domain, frequency-domain, and linear and non-linear features.

The complexity of these features can range from basic statistical measures like mean, median, minimum, and maximum to more intricate features based on specific data modalities. Each used in stress detection may yield a unique set of features, contributing to the overall data analysis and model accuracy. The selection and application of these features are crucial, as they directly impact the classification stage, ultimately influencing the model's performance in stress recognition.

Comprehensive reviews have been conducted on this, notable Giannakakis et al. (2022), Arsalan et al. (2023). We have utilized these extensive analyses as a foundation to select and identify the appropriate features into our study.

4.3.1 BVP-Blood Volume Pressure

Photoplethysmography (PPG) sensors provide a non-invasive optical method to acquire Blood Volume Pulse (BVP) signals, detecting volumetric blood flow changes as explained 2.3.1. Among the various metrics that can be extracted from PPG signals, Heart Rate (HR) and Heart Rate Variability (HRV) are prominent. These features offer critical insights into cardiac function and stress response. Detailed discussion of HR and HRV feature extraction from PPG will follow later.

After initial pre-processing of the PPG signal, which includes filtering, baseline correction, normalization, and signal quality assessment, the pivotal step in signal analysis is peak detection. This involves accurately identifying systolic peaks in the blood volume pulse, crucial for calculating HR and HRV as well.

The PPG waveform typically comprises two peaks: systolic and diastolic. While systolic peaks are usually prominent, diastolic peaks may not be observable in certain conditions. However, when identifiable, diastolic peaks offer additional information, contributing to a more comprehensive analysis.

To locate the diastolic peak, analysis often involves examining the first and second derivatives of the PPG signal, known as the Velocity Plethysmogram (VPG) and Acceleration Plethysmogram (APG), respectively (Suboh et al. 2022). Identifying fiducial points on VPG and APG is critical, as these points can provide insights into blood pressure estimation and other advanced cardiovascular analyses.

PPG signal analysis encompasses a variety of features across different domains:

Time Domain/Morphological Features : These features are directly extracted from the morphology (shape and structure) of the PPG waveform. These include cycle duration, peak amplitudes, and ratios of different waveform components. These features give insights into the blood volume changes with each heartbeat and can indicate changes in peripheral blood flow dynamics.

Frequency Domain Features : Analysis of the frequency components of the PPG/BVP signals reveals the rhythmic patterns linked to cardiovascular dynamics. This typically involves power spectrum analysis to identify dominant frequencies.

Statistical Features : The statistical analysis of PPG/BVP signals includes calculating mean, standard deviation, skewness, and kurtosis, offering a comprehensive statistical

overview of the waveform. Advanced Feature Extraction through VPG and APG Analysis further deepens the understanding of cardiovascular dynamics. These derivatives of the PPG signal expose intricate details about blood flow, particularly regarding systolic and diastolic activities. Features derived from VPG and APG include amplitudes and durations of specific waves and ratios comparing different waveform components.

HR Features

Heart Rate (HR) is a fundamental measure in cardiovascular and stress-related studies, representing the frequency of the heartbeat. It is considered to be the most widely adopted and straightforward measure to estimate stress levels (Giannakakis et al. 2022). It is typically expressed in beats per minute (bpm). The primary method of deriving HR from PPG involves counting the number of systolic peaks within a specified time frame.

Key Features and Analysis in HR:

- **Mean and Standard Deviation of the R-R Interval:** Provide a basic understanding of heart rate variability. The mean R-R interval offers insight into average heart rate, while the standard deviation reflects the variability around this mean.
- **Root Mean Square of the Successive Differences (RMSSD):** Measures the short-term variability in R-R intervals, primarily reflecting parasympathetic nervous system activity.
- **Mean R Peak Amplitude:** The average amplitude of the R peaks in the PPG signal, indicating the strength and consistency of heartbeats.
- **Skewness and Kurtosis of R-R Intervals:** Statistical measures describing the distribution of R-R intervals. Skewness indicates asymmetry, while kurtosis indicates the 'tailedness' of the distribution.
- **Percentile of R-R Intervals:** Involves calculating specific percentiles (e.g., 50th, 95th) of the R-R interval distribution, providing additional insights into heart rate variability.

HRV Features

Heart Rate Variability (HRV) analysis, an essential aspect of cardiac function understanding, is also derivable from PPG signals. HRV refers to the variation in the time interval between heartbeats, indicated by the beat-to-beat (R-R) intervals variation. It extends beyond a mere measure of cardiac rhythm, serving as an indicator of physiological resilience and adaptability in response to stress. HRV features extracted from PPG, including R-R interval and the root mean square difference of consecutive R-R intervals, are instrumental in assessing both heart rate dynamics and autonomic nervous system regulation.

Some of the key features in HRV analysis include:

Time-Domain Features

- **SDNN (Standard Deviation of NN intervals):** Measures overall heart rate variability.
- **RMSSD (Root Mean Square of Successive Differences):** Reflects the beat-to-beat variance in heart rate and is particularly sensitive to changes in the parasympathetic nervous system.
- **NN50 and pNN50:** NN50 counts the number of pairs of successive NN intervals differing by more than 50 ms, and pNN50 is the proportion of NN50 to the total number of NN intervals.

Frequency-Domain Features

- **Low Frequency (LF):** Represents a blend of sympathetic and parasympathetic activity.
- **High Frequency (HF):** Primarily reflects parasympathetic activity.
- **LF/HF Ratio:** Used to assess the balance between sympathetic and parasympathetic nervous systems.

Non-Linear Features

- **SD1/SD2 (Poincaré Plot Analysis):** Provides a geometric representation of HRV, offering insights into the complexity of heart rate dynamics.
- **Sample Entropy:** Measures the complexity or irregularity of R-R interval time series.

4.3.2 EDA-Electrodermal Activity

Electrodermal Activity (EDA), also known as galvanic skin response (GSR), is an indicator of emotional and physiological arousal, primarily influenced by the Sympathetic Nervous System (SNS). It primarily consists of two components: tonic (Skin Conductance Level, SCL) and phasic (Skin Conductance Response, SCR). As already explained in Section 2.3.1 the tonic component represents baseline levels of skin conductance, reflecting slow changes in arousal state. The phasic component, on the other hand, captures rapid fluctuations in response to specific stimuli or events. Dawson, Schell, and Filion (2007).

After the usual process of filtering, baseline correction and normalizing the signal as well as checking the quality of the signal we first decompose the EDA signal into its tonic and phasic components using continuous decomposition analysis. This process allows us to separately analyze the steady-state (SCL) and transient (SCR) aspects of skin conductance. The decomposition is typically carried out either using a highpass or bandpass filtering techniques or a convex optimization algorithm cvxEDA (Greco et al. 2016), ensuring that each component accurately represents the underlying physiological processes.

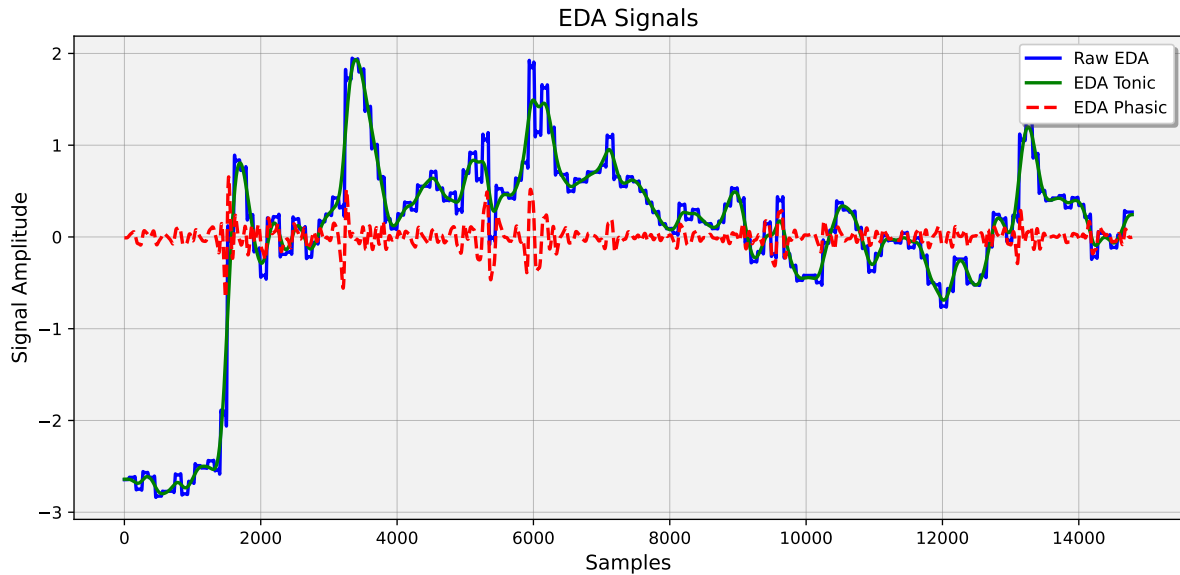


Figure 4.2: EDA

The activity of sweat glands, predominantly controlled by the SNS, leads to an increase in SCR during emotional arousal (Dawson, Schell, and Filion 2007). Notably, the non-specific SCR (NS.SCR) is intricately related to cognitive processes and psychophysiological states, acting as a direct measure of arousal (Nikula 1991). Unlike other physiological measures influenced by both sympathetic and parasympathetic nervous systems, SCR is exclusively modulated by the sympathetic nervous system, making it a reliable stress indicator (Setz et al. 2010). Under stress, both the tonic (SCL) and phasic (SCR) components escalate due to increased skin moisture (**stress**).

A thorough review and comparative analysis of various Electrodermal Activity (EDA) features have been conducted, as detailed by Shukla et al. (2021). This process involved a meticulous examination of close to 40 distinct EDA features previously identified in the literature. The outcome of this comprehensive analysis guided us in carefully selecting the features most necessary to the objectives of our research. Some of the key features from EDA include:

A detailed examination of the phasic component involves analyzing peak amplitude, frequency, and their inter-relationships in SCRs. This analysis is crucial for deciphering emotional and cognitive stress responses, as these metrics directly reflect the intensity and frequency of physiological reactions to stimuli.

From the decomposed EDA data, a variety of time domain statistical features can be extracted. These include mean (μ), standard deviation (σ), coefficient of variance (CV), variance (σ^2), and kurtosis (β) from the phasic component.

Mean (μ) provides a measure of the central tendency of the SCR amplitudes. Standard deviation (σ) and variance (σ^2) capture the variability or dispersion around the mean. The coefficient of variance (CV) offers a normalized measure of dispersion relative to the mean. Kurtosis (β) evaluates the peakedness or flatness of the distribution of SCR amplitudes. In addition to time-domain features, we analyze the EDA signal in the frequency domain. Furthermore, frequency-domain features like spectral power in specific bands (f1sc, f2sc,

f3sc) and the overall energy and entropy of the signal gave us a spectrum-based view of the EDA responses. By analyzing these features, we could discern patterns and rhythms in the EDA that are not immediately apparent in the time-domain.

Detecting and analyzing peaks in the phasic component (SCRs) is crucial. Peak amplitude, frequency, and their inter-relationships can be strong indicators of emotional and cognitive stress responses.

By examining both tonic and phasic components, we can understand the sustained arousal level (SCL) and the specific responses to stimuli (SCR). The correlation between these components can provide valuable insights into how sustained stress levels influence responses to immediate stimuli. From the tonic component, which encapsulates the underlying level of arousal, we calculated the mean, capturing the central tendency over time, and the standard deviation, offering insights into the variability around this mean. The maximum and minimum values, along with the range, provided us with the extremes of the EDA signal, painting a picture of the breadth of responses.

From the phasic component, we focused on the Skin Conductance Responses (SCRs) to discern more rapid changes associated with specific stimuli. We extracted features like SCR amplitude, which reflects the intensity of the response, and the frequency of these SCRs, indicating how often these responses occur. The kurtosis of SCR amplitudes, a measure of the 'tailedness' of the distribution, gave us an understanding of how peaked or flat the distribution of responses was, while the skewness indicated any asymmetry, offering clues about the predominant direction of the response distribution.

We also looked at the root mean square (SCR RMS), which is a measure of the signal's magnitude, providing a summative measure of the signal's complexity over a given period. The integral of the SCR signal (SCR Integral) was calculated to understand the total magnitude of these phasic responses over time. These features, alongside others like SCR momentum, which is akin to the second moment of the distribution, provided a comprehensive statistical breakdown of the phasic EDA signals.

4.3.3 Body Features

Since we captured human motion using the motion capture system, we selected 13 key points from the 25 marker points used by the system, focusing on the upper body. The chosen points were Hip, Ab, Chest, Neck, Head, Left Shoulder (LShoulder), Left Upper Arm (LUArm), Left Forearm (LFArm), Left Hand (LHand), Right Shoulder (RShoulder), Right Upper Arm (RUArm), Right Forearm (RFArm), and Right Hand (RHand). These points were strategically selected to comprehensively capture the whole upper body movements. The arrangement of these points is depicted in Fig 4.3

Self Touching

Giakoumis et al. (2012) has shown that body posture and body language can be valuable indicators of stress. In line with this, we also explored body language cues such as self-touching, which Harrigan (1985)suggests can be indicative of negative affect, such as anxiety or discomfort. Specifically, we focused on face and head touching as potential stress indicators.

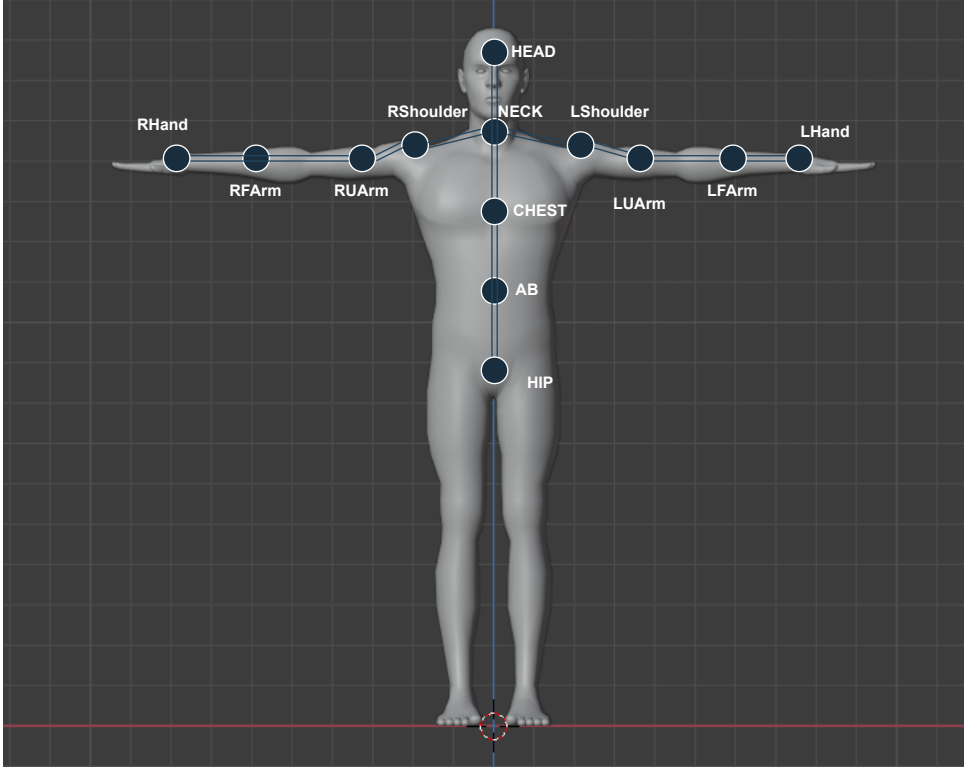


Figure 4.3: 13 points from the motion capture

To determine if a person is touching her face, we compute the hand-head and the hand-neck distances. If one of these distances is below a given threshold, we consider that the person is face touching. The number of occurrences (FTC) and the average duration (FTMD) of these face touching events are used as features.

To determine gestures such as face touching, $/tf$ data, which typically includes the position and orientation of each joint in space, can be utilized to calculate the distance between any two points. For example, if you have the coordinates of the right hand (RHand) and the head (HEAD), you can compute the Euclidean distance between these two points at each time frame to detect when the hand is close enough to the head to indicate potential face touching.

Let's define the 3D coordinates for the right hand and head at time t as:

- $P_{\text{RHand}}(t)$ for the position of the right hand at time t , with coordinates $(x_{\text{RHand}}(t), y_{\text{RHand}}(t), z_{\text{RHand}}(t))$,
- $P_{\text{HEAD}}(t)$ for the position of the head at time t , with coordinates $(x_{\text{HEAD}}(t), y_{\text{HEAD}}(t), z_{\text{HEAD}}(t))$.

The distance between the right hand and the head at time t is then calculated with the formula:

$$D_{\text{RHand-HEAD}}(t) = \sqrt{(x_{\text{RHand}}(t) - x_{\text{HEAD}}(t))^2 + (y_{\text{RHand}}(t) - y_{\text{HEAD}}(t))^2 + (z_{\text{RHand}}(t) - z_{\text{HEAD}}(t))^2} \quad (4.3.1)$$

If this distance, $D_{\text{RHand-HEAD}}(t)$, is less than a certain threshold, denoted as θ , it suggests that the right hand is in proximity to the head, indicating potential face touching.

To determine the occurrence of face touching, you would track when this distance becomes less than the threshold θ and also ensure that the hand remains within this threshold for a certain duration to count as an occurrence. The distance for the left hand can be calculated in a similar manner.

To compute the number of occurrences (*FTC-Face Touching Count*) and the average duration (*FTMD-Face Touching Mean Duration*) of face touching is shown in Algorithm 4.3.1.

Algorithm 4.3.1.: Face Touching Detection

Require: Set of time-stamped positions from the `/tf` topic, Threshold distance θ

```

1: function DETECTFACE TOUCHING
2:   Initialize  $FTC \leftarrow 0$                                  $\triangleright$  Occurrences of face touching
3:   Initialize  $TotalDuration \leftarrow 0$                        $\triangleright$  Total duration of face touching events
4:   Initialize  $FTMD \leftarrow 0$                                  $\triangleright$  Mean duration of face touching events
5:   for each time stamp  $t_i$  in /tf topic do
6:     Calculate  $D_{RHand-Head}(t_i)$  and  $D_{LHand-Head}(t_i)$ 
7:     if  $D_{RHand-Head}(t_i) < \theta$  or  $D_{LHand-Head}(t_i) < \theta$  then
8:       Start duration counter
9:        $FTC \leftarrow FTC + 1$ 
10:      if either distance exceeds  $\theta$  then
11:        Stop duration counter
12:        Add duration to  $TotalDuration$ 
13:      if  $FTC > 0$  then
14:         $FTMD \leftarrow \frac{TotalDuration}{FTC}$                        $\triangleright$  Calculate mean duration
15:   return  $FTC, FTMD$ 

```

Sudden Movement

Lagomarsino et al. (2022) suggests another way in which motion data can be used to assess stress that is by identifying periods of high activity/sudden activity called hyperactivity. Sudden movements, or abrupt changes in body motion, can be indicative of stress responses. These movements are characterized by significant deviations from a person's regular movement patterns and can be quantitatively assessed using motion capture data. The following equations describe the computational process used to analyze sudden movements and infer stress.

$$m_j^k = \sum_{i=0}^{\tau-1} d_j^{k-i, k-i-1} \quad (4.3.2)$$

Equation 4.3.2 defines the movement of the j^{th} joint within a time window τ as the sum of the displacements between consecutive frames.

$$\Delta_j^k = m_j^k - \mu_j \quad (4.3.3)$$

In Equation 4.3.3, Δ_j^k represents the deviation of the j^{th} joint's movement from its baseline mean motion μ_j , calculated during a calibration phase.

$$a_j^k = \begin{cases} \frac{\Delta_j^k}{\sigma_j} - 1 & \text{if } \Delta_j^k > \sigma_j \\ 0 & \text{otherwise} \end{cases} \quad (4.3.4)$$

Equation 4.3.4 assesses the activity level a_j^k for the j^{th} joint, taking into account the standard deviation σ_j as a threshold for sudden movement.

$$a_k = \min \left(1, \frac{1}{N} \sum_{j=1}^N a_j^k \right) \quad (4.3.5)$$

Finally, Equation 4.3.5 calculates the overall level of sudden movement at time instance k by averaging the activities across all joints, thus providing a descriptor of hyperactivity or sudden movement.

This method allows for a comprehensive analysis of the motion data to identify periods of high activity that may correlate with stress responses.

While our study focuses on the analysis of upper body movements for stress detection, it is important to note that other bodily cues can also be significant indicators of stress or anxiety. One such example is the rapid tapping or bouncing of one's feet, which is often a subconscious response to nervous energy or unease. Such movements are typically a form of self-soothing behavior that occurs when an individual is experiencing discomfort or stress.

Unfortunately, due to the scope of our study setup, we restricted our tracking to the upper body and therefore could not capture lower body movements, such as foot tapping or leg bouncing. These actions could potentially provide additional insights into a participant's stress levels and offer a more comprehensive understanding of physical stress responses.

Including lower body data in future studies could enhance the detection and analysis of stress indicators, allowing for a fuller picture of the physiological and behavioral state of an individual under stress. This would enable us to capture a wider range of stress-related behaviors and potentially increase the accuracy and reliability of stress detection in real-time scenarios.

4.4 Ground Truth

4.5 Classification /Stress Detection/

Feature	Full Name	Extracted From	Domain	Expected Behavior Under Stress
HR	Heart Rate	PPG-HR	Time Domain	Increase
MEAN IBI	Mean Interbeat Interval	PPG-HRV	Time Domain	Decrease
SDNN	Standard Deviation of NN intervals	PPG-HRV	Time Domain	Decrease
RMSSD	Root Mean Square of Successive Differences	PPG-HRV	Time Domain	Decrease
pNN50	Proportion of NN50 divided by total number of NNs	PPG-HRV	Time Domain	Decrease
Total Power	Total Power of HRV spectrum	PPG-HRV	Frequency Domain	Increase
VLF	Very Low Frequency	PPG-HRV	Frequency Domain	No Significant Change
LF	Low Frequency	PPG-HRV	Frequency Domain	Increase
HF	High Frequency	PPG-HRV	Frequency Domain	Decrease
LF/HF	Low Frequency/High Frequency ratio	PPG-HRV	Frequency Domain	Increase
SD1	Poincaré Plot Standard Deviation perpendicular to the line of identity	PPG-HRV	Non-Linear Domain	Varies
SD2	Poincaré Plot Standard Deviation along the line of identity	PPG-HRV	Non-Linear Domain	Varies
ApEn	Approximate Entropy	PPG-HRV	Non-Linear Domain	Varies
SampEn	Sample Entropy	PPG-HRV	Non-Linear Domain	Varies
SCL	Skin Conductance Level	EDA	Time Domain	Increase
SCPh	Phasic Skin Conductance Signal Power	EDA	Frequency Domain	Increase
SCRR	Number of Skin Conductance Responses	EDA	Frequency Domain	Increase
SCdiff2	Skin Conductance Level Deviation Squared	EDA	Time Domain	Increase
EDA Level	General Electrodermal Activity Level	EDA	Time Domain	Increase
Peak Amplitude	Maximum Amplitude of Skin Conductance Response	EDA	Time Domain	Increase
Rise Time to Peak	Time to Reach Peak Amplitude from Onset	EDA	Time Domain	Decrease/Varies
Decay Time	Time to Decrease from Peak Amplitude to Baseline	EDA	Time Domain	Increase/Varies
Half Recovery Time	Time for SCR Amplitude to Reduce to Half	EDA	Time Domain	Increase/Varies
Response Latency	Time between Stimulus Onset and Start of SCR	EDA	Time Domain	Increase/Varies
EDR Rate	Event-Related SCR Rate	EDA	Frequency Domain	Increase

Table 4.1: Physiological Markers for Stress Detection in PPG and EDA Signals

5

Result

6

Discussion and Conclusion

Bibliography

- Aigrain, J., M. Spodenkiewicz, S. Dubuisson, M. Detyniecki, D. Cohen, and M. Chetouani (2018):** “Multimodal Stress Detection from Multiple Assessments”. In: *IEEE Transactions on Affective Computing* 9.4, pp. 491–506.
- Alexander, D. M., C. Trengove, P. Johnston, T. Cooper, J. August, and E. Gordon (2005):** “Separating individual skin conductance responses in a short interstimulus-interval paradigm”. In: *Journal of neuroscience methods* 146.1, pp. 116–123.
- Arsalan, A., M. Majid, I. F. Nizami, W. Manzoor, S. M. Anwar, and J. Ryu (June 2023):** *Human Stress Assessment: A Comprehensive Review of Methods Using Wearable Sensors and Non-wearable Techniques*. en. arXiv:2202.03033 [cs]. URL: <http://arxiv.org/abs/2202.03033> (visited on 02/02/2024).
- Badillo, S., B. Banfai, F. Birzele, I. I. Davydov, L. Hutchinson, T. Kam-Thong, J. Siebourg-Polster, B. Steiert, and J. D. Zhang (Apr. 2020):** “An introduction to machine learning”. en. In: *Clin. Pharmacol. Ther.* 107.4, pp. 871–885.
- Bhushan, U. and S. Maji (2023):** “Prediction and Analysis of Stress Using Machine Learning: A Review”. In: *Proceedings of Third Doctoral Symposium on Computational Intelligence*, pp. 419–432.
- Bradley, M. M. and P. J. Lang (1994):** “Measuring emotion: The self-assessment manikin and the semantic differential”. In: *Journal of Behavior Therapy and Experimental Psychiatry* 25.1, pp. 49–59. URL: <https://www.sciencedirect.com/science/article/pii/0005791694900639>.
- Brantley, P. J., C. D. Waggoner, G. N. Jones, and N. B. Rappaport (Feb. 1987):** “A Daily Stress Inventory: development, reliability, and validity”. en. In: *J. Behav. Med.* 10.1, pp. 61–74.
- Cohen, S., T. Kamarck, and R. Mermelstein (1983):** “A Global Measure of Perceived Stress”. In: *Journal of Health and Social Behavior* 24.4, pp. 385–396. URL: <http://www.jstor.org/stable/2136404> (visited on 02/11/2024).
- Dawson, M. E., A. M. Schell, and D. L. Filion (2007):** “The electrodermal system.” In: *Handbook of psychophysiology*, 3rd ed. Pp. 159–181.
- Empatica (n.d.[a]):** *Empatica E4*. Available under: <https://e4.empatica.com/e4-wristband>.
- Empatica (n.d.[b]):** *Empatica E4 specs*. Available under: https://box.empatica.com/documentation/20141119_E4_TechSpecs.pdf.

- Empatica (n.d.[c]):** *Utilizing the PPG/BVP signal.* Available under: <https://support.empatica.com/hc/en-us/articles/204954639-Utilizing-the-PPG-BVP-signal>.
- Garbarino, M., M. Lai, D. Bender, R. Picard, and S. Tognetti (Jan. 2015):** “Empatica E3 - A wearable wireless multi-sensor device for real-time computerized biofeedback and data acquisition”. In: pp. 39–42.
- Gedam, S. and S. Paul (2021):** “A Review on Mental Stress Detection Using Wearable Sensors and Machine Learning Techniques”. en. In: *IEEE Access* 9, pp. 84045–84066. URL: <https://ieeexplore.ieee.org/document/9445082/> (visited on 02/02/2024).
- Gellman, M. D. (2020):** “Behavioral medicine”. In: *Encyclopedia of behavioral medicine*, pp. 223–226.
- Giakoumis, D., A. Drosou, P. Cipresso, D. Tzovaras, G. Hassapis, A. Gaggioli, and G. Riva (Sept. 2012):** “Using Activity-Related Behavioural Features towards More Effective Automatic Stress Detection”. In: *PLOS ONE* 7.9, pp. 1–16. URL: <https://doi.org/10.1371/journal.pone.0043571>.
- Giannakakis, G., D. Grigoriadis, K. Giannakaki, O. Simantiraki, A. Roniotis, and M. Tsiknakis (Jan. 2022):** “Review on Psychological Stress Detection Using Biosignals”. In: *IEEE Transactions on Affective Computing* 13.1. Conference Name: IEEE Transactions on Affective Computing, pp. 440–460. URL: <https://ieeexplore.ieee.org/document/8758154> (visited on 01/08/2024).
- Greco, A., G. Valenza, A. Lanata, E. P. Scilingo, and L. Citi (2016):** “cvxEDA: A Convex Optimization Approach to Electrodermal Activity Processing”. In: *IEEE Transactions on Biomedical Engineering* 63.4, pp. 797–804.
- Harrigan, J. A. (1985):** “Self-touching as an indicator of underlying affect and language processes”. In: *Social Science and Medicine* 20.11, pp. 1161–1168. URL: <https://www.sciencedirect.com/science/article/pii/0277953685901935>.
- Hart, S. G. and L. E. Staveland (1988):** “Development of NASA-TLX (Task Load Index): Results of Empirical and Theoretical Research”. In: *Human Mental Workload*. Vol. 52. Advances in Psychology, pp. 139–183. URL: <https://www.sciencedirect.com/science/article/pii/S0166411508623869>.
- Hernando-Gallego, F., D. Luengo, and A. Artés-Rodríguez (2017):** “Feature extraction of galvanic skin responses by nonnegative sparse deconvolution”. In: *IEEE journal of biomedical and health informatics* 22.5, pp. 1385–1394.
- imotions (n.d.):** *EDA Example signals.* Available under: <https://imotions.com/blog/learning/research-fundamentals/eda/>.
- Koverola, M., A. Kunnari, J. Sundvall, and M. Laakasuo (June 2022):** “General Attitudes Towards Robots Scale (GAToRS): A New Instrument for Social Surveys”. In: *International Journal of Social Robotics* 14, pp. 1–23.

- Krämer, M., C. Rösmann, F. Hoffmann, and T. Bertram (2020):** “Model predictive control of a collaborative manipulator considering dynamic obstacles”. In: *Optimal Control Applications and Methods* 41.4, pp. 1211–1232. eprint: <https://onlinelibrary.wiley.com/doi/pdf/10.1002/oca.2599>. URL: <https://onlinelibrary.wiley.com/doi/abs/10.1002/oca.2599>.
- Lagomarsino, M., M. Lorenzini, E. De Momi, and A. Ajoudani (2022):** “An Online Framework for Cognitive Load Assessment in Industrial Tasks”. In: *Robotics and Computer-Integrated Manufacturing* 78, p. 102380. URL: <https://www.sciencedirect.com/science/article/pii/S0736584522000679>.
- Larsen, E., S. Gottschalk, M. Lin, and D. Manocha (Dec. 2000):** “Fast Proximity Queries with Swept Sphere Volumes”. In.
- Lasota, P. A. and J. A. Shah (2015):** “Analyzing the Effects of Human-Aware Motion Planning on Close-Proximity Human–Robot Collaboration”. In: *Human Factors* 57.1. PMID: 25790568, pp. 21–33.
- Lee, M.-h., G. Yang, H.-K. Lee, and S. Bang (2004):** “Development stress monitoring system based on personal digital assistant (PDA)”. In: *The 26th Annual International Conference of the IEEE Engineering in Medicine and Biology Society*. Vol. 1. IEEE, pp. 2364–2367.
- Machado-Moreira, C., J. Caldwell Odgers, I. Mekjavić, and N. Taylor (Dec. 2008):** “Sweat Secretion from Palmar and Dorsal Surfaces of the Hands During Passive and Active Heating”. In: *Aviation, space, and environmental medicine* 79, pp. 1034–40.
- Nahavandi, S. (2019):** “Industry 5.0—A Human-Centric Solution”. In: *Sustainability* 11.16. URL: <https://www.mdpi.com/2071-1050/11/16/4371>.
- Nguyen, T. and Y. Zeng (Oct. 2017):** “Effects of stress and effort on self-rated reports in experimental study of design activities”. In: *Journal of Intelligent Manufacturing* 28.
- Nikula, R. (1991):** “Psychological Correlates of Nonspecific Skin Conductance Responses”. In: *Psychophysiology* 28.1, pp. 86–90. eprint: <https://onlinelibrary.wiley.com/doi/pdf/10.1111/j.1469-8986.1991.tb03392.x>. URL: <https://onlinelibrary.wiley.com/doi/abs/10.1111/j.1469-8986.1991.tb03392.x>.
- OptiTrack (n.d.):** *Motive Skeleton Tracking*. Available under: <https://docs.optitrack.com/motive/skeleton-tracking>.
- Pandian, V. and S. Suleri (Jan. 2020):** *NASA-TLX Web App: An Online Tool to Analyse Subjective Workload*.
- Pereira, R. and N. dos Santos (2023):** “Reflections on a New Paradigmatic Approach for the Industry: A Scoping Review on Industry 5.0”. In: *Logistics* 7.3. URL: <https://www.mdpi.com/2305-6290/7/3/43>.

- Renz, H., M. Krämer, and T. Bertram (2023a):** “Comparing Human Motion Forecasts in Moving Horizon Trajectory Planning of Collaborative Robots”. In: *2023 IEEE International Conference on Robotics and Biomimetics (ROBIO)*, pp. 1–6.
- Renz, H., M. Krämer, and T. Bertram (2023b):** “Uncertainty Estimation for Predictive Collision Avoidance in Human-Robot Collaboration”. In: *2023 IEEE International Conference on Robotics and Biomimetics (ROBIO)*, pp. 1–6.
- Roberts, V. (1982):** “Photoplethysmography- fundamental aspects of the optical properties of blood in motion”. In: *Transactions of the Institute of Measurement and Control* 4.2, pp. 101–106. eprint: <https://doi.org/10.1177/014233128200400205>. URL: <https://doi.org/10.1177/014233128200400205>.
- Sauppé, A. and B. Mutlu (2015):** “The Social Impact of a Robot Co-Worker in Industrial Settings”. In: URL: <https://doi.org/10.1145/2702123.2702181>.
- Schulz, P. and W. Schlotz (Jan. 1999):** “The Trier Inventory for the Assessment of Chronic Stress (TICS): Scale construction, statistical testing, and validation of the scale work overload”. In: *Diagnostica* 45, pp. 8–19.
- Setz, C., B. Arnrich, J. Schumm, R. Marca, G. Tröster, and U. Ehlert (Jan. 2010):** “Discriminating stress from cognitive load using a wearable EDA device.” In: *IEEE Transactions on Information Technology in Biomedicine* 14, pp. 410–417.
- Sharma, N. and T. Gedeon (Dec. 2012):** “Objective measures, sensors and computational techniques for stress recognition and classification: a survey”. en. In: *Comput. Methods Programs Biomed.* 108.3, pp. 1287–1301.
- Shukla, J., M. Barreda-Ángeles, J. Oliver, G. C. Nandi, and D. Puig (2021):** “Feature Extraction and Selection for Emotion Recognition from Electrodermal Activity”. In: *IEEE Transactions on Affective Computing* 12.4, pp. 857–869.
- Suboh, M. Z., R. Jaafar, N. A. Nayan, N. H. Harun, and M. S. F. Mohamad (2022):** “Analysis on Four Derivative Waveforms of Photoplethysmogram (PPG) for Fiducial Point Detection”. In: *Frontiers in Public Health* 10. URL: <https://www.frontiersin.org/articles/10.3389/fpubh.2022.920946>.
- Vos, G., K. Trinh, Z. Sarnyai, and M. Rahimi Azghadi (May 2023):** “Generalizable machine learning for stress monitoring from wearable devices: A systematic literature review”. en. In: *International Journal of Medical Informatics* 173, p. 105026. URL: <https://linkinghub.elsevier.com/retrieve/pii/S1386505623000436> (visited on 01/10/2024).
- Zakeri, Z., A. Arif, A. Omurtag, P. Breedon, and A. Khalid (Oct. 2023):** “Multimodal assessment of cognitive workload using neural, subjective and behavioural measures in smart factory settings”.
- Zhang, Q., L.-G. Lindberg, R. Kadefors, and S. Jorma (May 2001):** “A non-invasive measure of changes in blood flow in the human anterior tibial muscle”. In: *Arbeitsphysiologie* 84, pp. 448–452.

7

Appendix

Das ist der Anhang (siehe Abschnitt ??) / This is the appendix (see section ??)

7.1 Usage of generative AI - Affidavit

- not at all
- for correcting, optimizing, or restructuring the entire work (This eliminates the need for explicit marking of individual passages or sections, as this type of usage refers to the entire written work. Explicit marking in the text is not necessary, as this serves as the global indication.)
- Code optimization: Optimization or restructuring of software function
- Code generation: Creating entire software functions from a detailed functional description.
- Substance generation in code: Generating entire software source code
- Media optimization: Correction, optimization, or restructuring of entire passages
- Media generation: Creating entire passages from given content.
- Substance generation in media: Generating entire sections
- More, namely:

I assure that I have provided all usages completely. Missing or incorrect information may be considered an attempt to deceive.

place, date

Jane Doe